What makes fish school?

An approach to mathematical modelling and simulation of fish schooling that enables incorporation of experimental data

Lisette de Boer

August 16, 2010

Master Thesis Lisette de Boer
Mathematical Institute, Leiden University
Thesis Supervisor: Dr. S.C. Hille

Mathematisch Instituut, Universiteit Leiden

Preface

In this thesis we investigate the collective behaviour of fish called schooling. It is written around one central question: how does this schooling behaviour arise from individual response to the observed environment? We investigated how this can be modelled mathematically in such a way that there is an explicit and precisely formulated relationship to relevant biological and (bio)physical processes. There already exist mathematical models to simulate aggregation behaviour. Most of these models however do not properly relate to the underlying biology. For example, some important physical properties of the sensory systems of fish have not been taken into account in these models, like the fact that neighbouring fish might be hidden behind each other, that water quality might influence the vision of fish and that fish typically do not see depth and hence are not able to determine the absolute distance to their neighbours. Hence, most models lack validation by experiment. Actually, their poor relation to the biology inhibits validation.
In this thesis we propose an approach to the modelling and subsequent simulation and analysis of the collective behaviour, in which we carefully separate an individual's observation of the environment, decision making and the subsequent physical response. What the organism can observe is accessible to biophysical and chemical considerations and experiment. Moreover, their physical response is also accessible in such a way. When we relate this to our central question, we find that the functioning of the fish's decision system, which links observation and response, is of critical importance in resolving it. It obviously is poorly accessible to experiment, but in order to get some insight, it is important to realize that as input one should take what an individual *can observe*, and as an output how it physically *can respond*.
We have made a mathematical model based on existing models, but with a relation to biology along the line sketched above, which can be linked to experimental data and be executed together with experiments to explain behaviour from hypotheses on how the decision system relates observation to response. The execution of the experiments itself was beyond the scope of this thesis in (bio)mathematics. We expect that future experimental work in conjunction with the type of mathematical modelling and simulation proposed here will yield new and deeper insights in the question how fish school and what the important parameters are which determine the characteristics of the resulting school.
The model incorporates different aspects to take into account the points of criticism mentioned above. We will investigate how observation, memory, decision and response are intertwined and unravel the relation between them in the model. These parts are recognizable in the structural set-up of the high-level architecture of our model. This high level 'model architecture' is not limited to the study of fish schooling. It is relevant and useful for different organisms. In particular, it is interesting to "put it to the test" with e.g. unicellular organisms like bacteria, amoebae or macrophages in the immune system. These have the advantage that their decision making system should be less complicated compared to higher organisms, like fish. Moreover, these model systems seem to be more easily accessible experimentally.
We will make a comparison to existing models and investigate possible differences.

In this thesis we set out to develop, implement and try-out a modelling and simulation approach, that has the potential of bringing mathematics, physics and experimental biology closer together on the topic of understanding collective behaviour of organisms. To succeed, the challenge is not to excel and go deep in one of these fields, but to understand all at a proper level and find the best combination of these fields in order to truly assess the question. Our biggest challenge has been to collect and combine the large variety of subjects needed for this research, for which we have investigated different parts of mathematics, physics and biology.
We hope the reader will enjoy this combination of topics as we did and will be convinced of the necessity of the proposed approach in order to establish a better, i.e. more explicit and experimentally accessible, relationship to biology in the field of modelling, simulation and analysis of collective behaviour of living organisms and artificial agents like robots, in the future.

Lisette de Boer

Contents

Chapter 1

Introduction

There is a long lasting interest in the collective behaviour of living organisms. A question of particular interest was, whether or not an intelligent leader was required to coordinate group behaviour or aggregation of individuals. Since the beginning of 1950 the behaviour patterns of different species have been investigated using mathematical models. Among others, one studied group behaviour of e.g. ants, birds (in particular starling), and fish, see Figure 1.1. In this thesis we shall consider the mathematical modelling and simulation of fish schooling.

Figure 1.1: Examples of collective behaviour of starling, army-ants and bigeye trevally

1.1 The biology and physics of fish swimming

There are more than 25.000 different species of fish known so far. There are more kinds of fish than all other vertebrates together. Over 95% of all living fish today are bony teleosts. About 50%-80% of fish swim in *schools* [5]. A school is defined as a group of fish that are swimming at about the same speed in roughly parallel orientation and maintaining a constant distance to their nearest neighbour. A school contains fish of about the same size: individuals that differ in size around 30% simply do not fit in. A *shoal* is a social group, but not necessarily a school because fish in a shoal may have random orientation, nearest neighbour distance and sizes. It has been suggested that schooling and other forms of social shoaling play important roles in searching for food, predator avoidance and energy conservation [5].
There are different types of fish. We will investigate *pelagic* fish, which live in

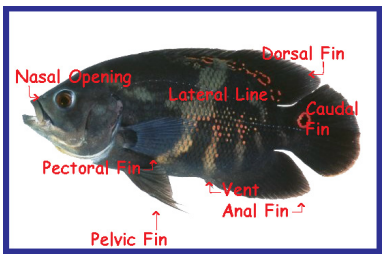

Figure 1.2: Fish

an open part of the sea or ocean, in the middle of the water column between the surface and the bottom of a sea or lake. These fish can be contrasted with *demersal* fish, which live on or near the bottom of an ocean or lake, and *reef* fish which live in coral reefs. Pelagic fish can be divided in two groups: *coastal* (or inshore), and *oceanic* (or offshore). We will investigate the latter.
Fish can use different methods for swimming. They use their fins in one way or another, depending on the type of fish, to propulse themselves through the water, [21]. In Figure 1.2 it is described how the different fins are located at the body of the fish. As we will see later on, oceanic pelagic fish will mainly use their tail or caudal fin as the main propulsive and steering device. For other kinds like coastal and reef fish, other fins may be more important for steering.
One makes the distinction between neutrally, negatively and positively buoyant. When a fish is more dense than water it is negatively buoyant, which means that (part of) its body will sink. The fish use different methods to maintain at the same level in the water. For example, they may use their pectoral fins as lifting foils. If only the tail part of the body sinks, this generates a dynamic lift when swimming. These types of fish tend to use the so called *kick-and-glide* method: by alternating propulsive body movements and periods of gliding they are able to save 20% or more energy, [5, Ch 3 and 4]. The downside of being negatively buoyant is that these fish must maintain a minimum cruising speed to prevent them from sinking. Thus they have to be on the move constantly.
There are two ways a fish can create a static lift. The first is by gas and the second by fats and oils. Fish have a gas bladder which is about 5% of their body. By constantly secreting and absorbing gas they keep the volume of this bladder constant to remain neutrally bouyant. This way fish are able to regulate their buoyance very quickly. As second method fish use fats and oils as a source to generate static lift. An advantage of using lipids is that the density at the water surface barely differs from the density at the bottom of the sea. On the other hand, fish will find it difficult to adjust its density rapidly to cope with the short-term density changes resulting from feeding and parturition (laying eggs) [5].

1.2 Current theory on fish schooling

In [11], Huth and Wissel introduced rules of how fish may react to their environment and in [12] they continued this approach. Their way of describing the schooling rules for fish has been fully adopted by subsequent researchers.

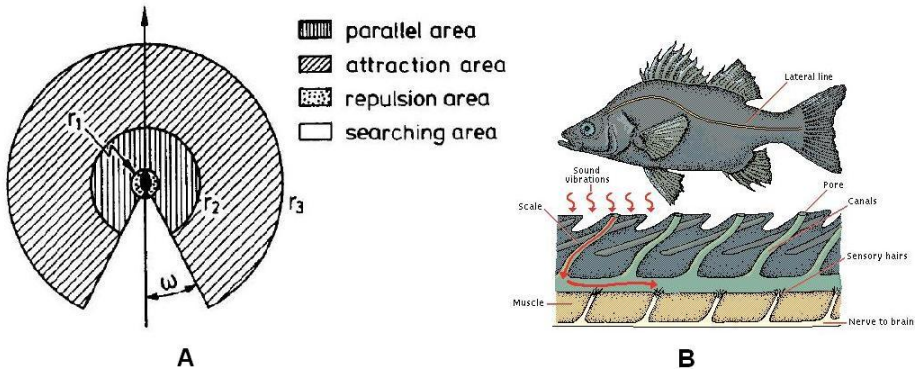

Figure 1.3: A: Different regions around the fish according to Huth and Wissel, [11]. B: The lateral lining system of fish.

According to Huth and Wissel, four different regions around the fish are relevant: the zone of repulsion, alignment and attraction, and the remaining part of their habitat designated as searching area. In Figure 1.3A it is shown how these regions are located around the fish, where the parallel area represents the alignment zone. Typical sizes for the radii of these zones expressed in the unit 'Body Length'(BL), are respectively $0.5BL, 2BL$ and $5BL$.
Fish use vision and their lateral line to observe the environment. The lateral line is an organ on the side of the body which senses movement and vibration in the surrounding water, see Figure 1.3B. Fish seem to use the lateral line to avoid collision and to realise alignment at short ranges, whereas vision is used to detect others at larger distance. Vision is important in schooling, since a school falls apart at night due to vision loss. When the lateral line is cut, fish swim closer to each other than the usual 1 to 1.5 BL distance.

1.3 A sketch of the history of modelling and simulation

From the 1990's computers were used to simulate schooling behaviour. In the first simulations, fish were just points in two-dimensional space which moved with constant speed. In [10] this speed has been made adjustable while an average cruising speed was maintained, possibly dependent on environmental and/or physiological state of the fish. This idea seems not to have been explored further, but we will investigate this approach further in this thesis.
In recent models, the two dimensional setting has been replaced by more realistic simulations in three dimensions, although mostly with periodic boundary conditions in all direction (if the boundary conditions are specified at all). This means that fish which swim out on one side, will enter again on the other side, in all directions. Incorporation of boundaries as water surface and sea floor seems to be rare. We will incorporate these in our approach to explore any possible effects of these boundary conditions.
There are models where also the size and shape of the fish are incorporated. In

[8] it was studied for the first time how body size and shape affect the shape of the school. We will also incorporate body size in our approach.

1.3.1 Discrete-time models

There are different ways of modelling fish behaviour. In [17] the authors have included a table which summarizes fish school simulation parameters and output variables from different researchers up to 1999. Here we give a few other examples of discrete-time models, followed in the next section by continuous-time models.

Couzin and coworkers
An example of a discrete-time model based on the absolute distance between fish is the model of Couzin *et al.* in [7]. Their aim is to provide new insights into the mechanism of effective leadership and decision-making in biological systems. They have adopted the different interaction zones described in [11] while postulating interaction rules in these zones. These rules do not seem to have been validated experimentally.
Each fish has a position $c_i(t)$ in three-dimensional space at time t. If there are neighbours in the zone of repulsion, the desired direction for fish i at the next time step is given by

$$d_i(t+1) = -\sum_{j=1}^{n} \frac{c_j(t) - c_i(t)}{|c_j(t) - c_i(t)|}. \tag{1.3.1}$$

where the summation runs over the neighbours in the zone of repulsion.
If there are no neighbours in the repulsion zone, fish in the alignment zone are taken into account. Then the desired direction is given by

$$d_i(t+1) = \sum_{j=1}^{n} \frac{v_j}{|v_j|} \tag{1.3.2}$$

where v_j represents the velocity of fish j, and the summation runs over all fish in the alignment zone.
Finally, if there are no other fish in the repulsion and alignment zone, they use the follow rule for attraction by their neighbours:

$$d_i(t+1) = \sum_{j=1}^{n} \frac{c_j(t) - c_i(t)}{|c_j(t) - c_i(t)|}. \tag{1.3.3}$$

If there are neighbours in both of the last two zones, these rules will be combined, simply by addition. Finally, the vector d_i will be converted into the unit vector $\hat{d}_i$. As may be clear from the equations above, this model does not incorporate any biological (experimental) data[1].
In [7], they investigate how many informed individuals are needed to guide a group. An informed individual has a nonzero vector $\vec{g}_i$ pointing in the 'informed

[1] We will provide an adjustment to this model at this point in Section 4

direction'. They introduce a weighting factor ω and incorporate the information g_i into the desired direction as an additional ω-weighted term:

$$d_i'(t+1) = \frac{\hat{d}_i(t+1) + \omega g_i}{|\hat{d}_i(t+1) + \omega g_i|}. \tag{1.3.4}$$

If $\omega = 0$, none of the individuals is informed about where to go. They reveal that the larger the group, the smaller the proportion of informed individuals needed to guide the group. However, these results only hold for their artificial interaction rules. They do not specify the 'virtual tank' they work in or any boundary conditions.

Hemelrijk and coworkers

In [9], Hemelrijk and Hildebrandt refined the situation of Huth and Wissel as described in Figure 1.3, see Figure 1.4. Here, the blind zone behind the fish is larger for the cohesion zone than for the repulsion zone and the alignment zone, because in former studies only vision is used, whereas in [9] the lateral line also plays part in determining these zones. They assume that the perceptual field of the lateral line follows the body form: therefore the repulsion and alignment regions are elliptical rather than circular [8].

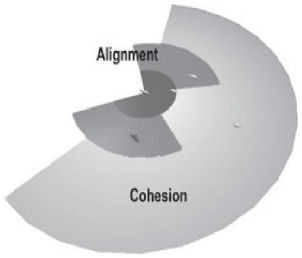

Figure 1.4: Regions refined by Hemelrijk and Hildebrandt, [9].

Most models are formulated in terms of the distances between the centres of mass of the fish. Hemelrijk's discrete-time model is based on the aggregation rules described by Couzin in [7]. In addition, fish in a school are also attracted to the centre of gravity of a group of individuals located in their attraction range. They mention that they have used a efficient spatial search method based on a Hilbert R-tree to locate their neighbours. A Hilbert R-tree is a tree data structure to store multidimensional objects such as lines and regions.
In [8], Hemelrijk and Hunz not only use the distance to the centre of mass of its neighbours, but also the distance to the nearest point. In [9] the previous model described in [8] has been improved by making it more realistic. The constant speed has been made variable and a 'cruise speed' has been introduced. Their aim is to develop testable hypotheses for the mechanisms underlying school shape and structure in real schools of fish.
Their virtual fish swim in a continuous, unbounded 3D world. They have developed detailed model-based hypotheses that may be used to verify whether in real fish an oblong school form and high frontal density appear as a side-effect of coordination in a similar way as in the model. Their model resulted in a oblong school with highest density at the front of the school which they investigated at

different group sizes and speed. They note a few shortcomings of their model: it only studies the consequences of simple rules for coordination. Vision is identical around the axis of movement, which implies that width and height of the school are identical, which is often not true in nature [9,14]. Their hypotheses have not yet been verified by empirical scientists.

Barbaro and coworkers
In [1], Barbaro *et al.* model the spawning migration of the Icelandic capelin stock, *Mallotus villosus*, by using an interacting particle model with added environmental field. The capelin, see Figure 1.5, is an example of a species of pelagic fish which covers several hundred kilometers in the course of its migration.

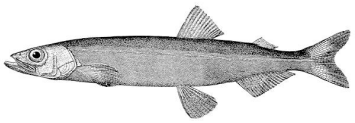

Figure 1.5: Capelin

The Icelandic fishing industry is interested in the capelin because it is a feeder fish for many larger, economically important species of fish such as cod and herring [2].
The interacting particle model is related to Couzin's model and based on the work of Hubbard and coworkers, which originated from work by Vicsek *et al.* [2,10,20]. Since the type of fish is specified and environmental aspects are added, this model is more realistic. But, unlike the models seen before, they do not employ a blind region behind a fish. They note that is ambiguous whether or not this blind zone is biologically relevant in the case of fish since the lateral line should allow a fish to sense the region behind it as it swims. To us it seems that for the largest range, the range of attraction, vision is the dominant sensory system. Then the blind zone is present and may have an effect. However, in their simulation, the presence of such a region does not seem to affect the outcome of the simulations [12].
Their model is two-dimensional in which particles update their speed v_i and their position q_k as follows

$$v_k(t+\Delta t) = \frac{1}{|O_k|}\sum_{j\in O_k} v_j(t) \tag{1.3.5}$$

$$\mathbf{q}_k(t+\Delta t) = \mathbf{q}_k(t) + \Delta t \cdot v_k(t+\Delta t)\begin{pmatrix}\cos(\phi_k(t+\Delta t))\\ \sin(\phi_k(t+\Delta t))\end{pmatrix} \tag{1.3.6}$$

where $|O_k|$ denotes the number of particles in the orientation zone and $\phi_k(t)$ is the directional angle of particle k with respect to the positive x-axis. They note that since the information on position and direction of neighbouring particles can lead to conflict of interest, they use a weighted average to determine the

particles desired direction, $\phi_k(t+\Delta t)$, in the next time step according to

$$\begin{pmatrix}\cos(\phi_k(t+\Delta t))\\ \sin(\phi_k(t+\Delta t))\end{pmatrix} = \frac{\mathbf{d}_k(t+\Delta t)}{|\mathbf{d}_k(t+\Delta t)|} \tag{1.3.7}$$

where

$$\begin{aligned}\mathbf{d}_k(t+\Delta t) &:= \frac{1}{|R_k|+|O_k|+|A_k|}\times \\ &\left(\sum_{r\in R_k}\frac{\mathbf{q}_k(t)-\mathbf{q}_r(t)}{|\mathbf{q}_k(t)-\mathbf{q}_r(t)|}+\sum_{o\in O_k}\begin{pmatrix}\cos(\phi_k(t)\\ \sin(\phi_k(t))\end{pmatrix}+\sum_{a\in A_k}\frac{\mathbf{q}_a(t)-\mathbf{q}_k(t)}{|\mathbf{q}_a(t)-\mathbf{q}_k(t)|}\right)\end{aligned} \tag{1.3.8}$$

with $|R_k|, |A_k|$ the number of neighbours in the repulsion and attraction zone respectively.
By including an environmental grid containing information about the current and the temperature at regular intervals, particles are able to respond to their environment. The data contained in the grid allow each fish to be translated by the current and to adjust its direction depending on the temperature of the surrounding ocean [1]. The particles sense the surrounding temperature T according to the gradient of the function r:

$$r(T) := \begin{cases} -(T-T_1)^4 & \text{if} \quad T \le T_1 \\ 0 & \text{if} \quad T_1 \le T \le T_2 \\ -(T-T_2)^2 & \text{if} \quad T_2 \le T, \end{cases}$$

where T_1, T_2 are constants and $[T_1, T_2]$ is referred as the preferred temperature range. The current field is denoted by $\mathbf{C}$.
By including the environmental fields, equation (1.3.6) becomes

$$\mathbf{q}_k(t+\Delta t) = \mathbf{q}_k(t)+\Delta t\cdot v_k(t+\Delta t)\frac{\mathbf{D}_k(t+\Delta t)}{|\mathbf{D}_k(t+\Delta t)|}+\mathbf{C}(\mathbf{q}_k(t)), \tag{1.3.9}$$

where

$$\mathbf{D}_k(t+\Delta t) := (1-\beta)\frac{\mathbf{d}_k(t+\Delta t)}{|\mathbf{d}_k(t+\Delta t)|}+\beta\frac{\nabla r(T(\mathbf{q}_k(t)))}{|\nabla r(T(\mathbf{q}_k(t)))|}. \tag{1.3.10}$$

Here $\beta \in [0,1]$, the temperature weight factor, determines the reaction of each particle to the temperature and its neighbours.
New in this model is the introduction of *superindividuals*; particles do not automatically represent individual fish, but may also represent many particles together, e.g. a school, behaving in an identical manner as an individual. There are several scaling relations explained in their article to justify the use of these superindividuals.
A contribution of this paper is that they were able to qualitatively reproduce the spawning migrations of the capelin without an external forcing term.

1.3.2 Continuous-time models

Various attempts have been made to model schooling behaviour by using a continuous-time model. We mention a few below.

Bertozzi, D'Orsogna and coworkers
The model designed by Bertozzi and D'Orsogna *et al.* described in [15,16], differs from previously described models, since it only uses the regions of repulsion and attraction and does not take alignment into consideration. They model a non-linear system of self-propelled individuals interacting via a pairwise attractive and repulsive potential. In contrast with the previous models, this is a continuous-time model.
They discuss aggregation patterns and asymptotic behaviours by investigating robot swarming. The underlying idea is to simulate agent motion in a manner similar to the motion of swarm-animals like birds and fish in nature. To describe the motion of the discrete swarming agent i they use the following equations of motion

$$\frac{dx_i}{dt} = v_i, \tag{1.3.11}$$

$$m_i \frac{dv_i}{dt} = (\alpha - \beta|v_i|^2)v_i - \nabla_i U(x_i), \tag{1.3.12}$$

where

$$U(x_i) = \sum_{j \neq i} \left[C_r e^{|x_i - x_j|/l_r} - C_a e^{-|x_i - x_j|/l_a} \right] \tag{1.3.13}$$

is the general Morse potential. Here l_a, l_r represent the range of the attractive and the repulsive part of the potential and C_a, C_r their amplitudes. From equation (1.3.12) we notice that agents tend to swim close to the self-propelled speed $|v_i| = \sqrt{\alpha/\beta}$.
This model is 2D, does not take alignment into account and assumes that all individuals have the same mass: $m_i = m$ for all i. They also mention in [15] that $|v_i|^2 = \alpha/\beta$ does not hold for rigid body structures. As will be mentioned later on, we will model our fish as rigid bodies and hence this approach is not useful for us.

Barbaro, Birnir and coworkers
Another continuous-time model by Barbaro and coworkers, [2,4], is based on the discrete-time model similar to the described model above by Barbaro *et al.* to describe the motion of the capelin. Their goal was to create a model which can be used to estimate the location of the capelin stock at various times of the year. They derived a system of four ODE's

$$\begin{cases} \dot{r}_k &= v_k \cos(\phi_k - \theta_k) \\ r_k \dot{\theta}_k &= v_k \sin(\phi_k - \theta_k) \\ \dot{v}_k &= \frac{\alpha}{N^2} \sum_{j=1}^{N} v_j \sum_{j=1}^{N} \cos(\phi_j - \phi_k) - \alpha v_k \\ v_k \dot{\phi}_k &= \frac{\alpha}{N^2} \sum_{j=1}^{N} v_j \sum_{j=1}^{N} \sin(\phi_j - \phi_k). \end{cases}$$

Here the position of each fish has been expressed in polar coordinates r and θ, N represents the number of individuals and a turning rate α has been introduced, which they fix at 1. By noting that the capelin tends to stay close to the water surface, they justify the choice of a 2D model.

By using these ODE's, they numerically found stationary, migratory and circling behaviour in both the discrete and the ODE model and two types of swarming behaviour in the discrete model [2].
First they note that the different interaction zones can be implemented using potentials, but that these zones are not necessary to find simple behaviours exhibited by the model. By adding small deterministic perturbation to the last two equations above, they also found circling solutions. They showed that by only incorporating the alignment zone, they found the same result as when using the repulsion and attraction zones.
By assigning a "selfWeight" to each fish, they were able to take a preferred direction of each fish into account. This corresponds to the method used in the discrete-time model by Couzin *et al.* of incorporating informed individuals. They note that the selfWeight needed to be approximately 1.5-2 times the total number of fish to achieve a swarming solution. By decreasing the selfWeight, a stable swarming solution can be made migratory. When the selfWeight approaches one quarter or less of the total number of fish, the school assumes parallelism and travels in a well-defined direction, transitioning to a migratory solution.

1.4 Discussion

The biological literature seems to agree upon the roles of vision and lateral line in the various interaction zones as identified by Huth and Wissel [11]. One important comment can be made about all models discussed above: the specified rules implicitly need the assumption that fish are able to measure the *absolute* distance to their neighbours. This seems quite unrealistic, since fish like the capelin typically have one eye on either side of their body and hence are not able to see depth. Moreover, considering fish as point masses makes the model predictions in crowded situations questionable. Yet another possible effect relating to the functioning of the visional sensory system is the effect of water quality. This limits the effective range of vision and hence the ability to see neighbours. And what is the difference in perception of a large neighbour far away compared to a small neighbour, really close? These are all questions which have not been answered yet.

A few researchers make slight improvements; in [9] the authors note that individuals are unlikely to perceive those that are hidden behind others. They note that the range of observation is inversely related to the density of the school; the observation range is flexible. In other words: if a fish is located at the centre of the school, it is not able to see fish far away because its vision is blocked by its neighbours, whereas on the outside of the school the vision of the fish reaches further. This model has the best relation to biology of the models investigated in Section 1.3.
In [24] the authors mention that there is a limited number of neighbours influencing the decision of a fish. They concluded from their previous investigations in [23] that the number of influencing neighbours should be 16. They introduce a scaling function for the influence of these 16 neighbours; if the closest neighbour is too close, this will have a large impact on a fish and will result in repulsion.

Also, a very close nearest neighbour would likely obstruct a large percentage of a fish's field of view, making more distant school-mates more difficult to see. We will provide a different method to prevent a fish to spot neighbours hidden behind others, see Section 2.1.2.

In [24], the authors aim to leverage well known rules of physics to help codify the fish schooling problem mathematically, without sacrificing the behavioural realism too greatly. They suggest that one should definitely incorporate drag and acceleration, which we will do further on in our model. They note that it is unlikely that animals can judge the distance to a target with perfect precision, but they still assume that organisms use distance as a relevant measure of influence. According to them, since animals are not capable of perfect visual acuity, some investigators assume there will be a margin of error in the computation of the preferred distance to neighbours. This margin is commonly formalized as a finite region, the "neutral zone", where there is neither attraction nor repulsion. This is also known as the alignment zone in most articles, and from our point of view this does not change the fact that fish are probably not able to determine the absolute distance to their neighbours at all.

A lot of fish school simulations described in articles do not specify which fish they are simulating. Maybe the zone of repulsion, alignment and attraction are different for different kind of fish. And how about the blind zone behind the fish? Does this depend on the type? In [24] they do specify the type of fish simulated. Their simulations are based on measurements of giant danio (*Danio aequipinatus*) movements taken from companion schooling experiments, [23]. In their article they have added a table of parameters to justify the choices made in their model.

Most models work like the model of Couzin in [7]. This model determines where one fish will go in the next time step, by measuring all the distances to its neighbours and their velocity in a certain zone and averaging it. But how do we know if this is the way fish make their decisions? Again, here it is not taken into account that fish may have different sizes and might be hidden behind each other. In [1] they concluded that their contribution was that they were able to reproduce spawning migrations without external forces, but does this model just copy what fish do, or is it really based on movements of fish? In other words, what is the connection of the model to the biology?
We will react to this subject in detail in Section 2.1.2.

1.5 Our objectives

In the previous section we have discussed several models and noted on which points these models lack the relation with biology and can be improved. Therefore we have made a model which can be linked to experimental data and be executed together with experiments in order to explain schooling behaviour, based on existing models.
We will introduce a *perceived distance* which will be used instead of the absolute

distance to neighbours. We will describe a different way to store the information of a fish's environment, the so-called *sphere of perception*. Besides the way fish see their surroundings, we are also going to investigate how fish combine the different impulses from their surroundings. We will make it impossible for fish to detect (part of) neighbours hidden behind others. Moreover, we will incorporate the physics of fish swimming into their response to the observed environment.
We will further develop a general modelling framework for collective behaviour, which we shall explain in the next chapter. This framework is very useful, since it enables us to easily adapt our model to other organisms than fish.

Chapter 2

High-level model and simulation architecture

Before fish can decide how to respond to their environment, they first need to observe this environment. Then they need to use their observations and combine this with information from their memory to decide how to react. This is the framework of our model: a clear separation of the processes of observation, decision making and response, see Figure 2.1. In this section we will describe the parts of our framework in detail and explain how it is used in modelling and the implementation of our simulation. By using this framework and making it visible in our simulation, our simulator can be easily adapted to the organism investigated. Whether we investigate fish, *E. coli* bacteria or white blood cells, the framework remains the same. Of course, the biophysical or chemical mechanisms of observation and response and their characteristics will differ, which also holds for how decisions are made from observations.

2.1 The framework constituents

2.1.1 The environment

The environment of an organism depends on the type of organism. It may contain individuals of the same type, other species like predators and prey, concentration of chemicals, water temperature etc. All elements in the environment of an organism may have an influence on the way it will respond. As shown in Figure 2.1, the environment is used as the input of an organism's observation system and it changes over time due to for example changes in concentration of chemicals, or moving and interacting individuals. The observed environment is accessible by biophysical and chemical considerations and experiment and the physical response is also accessible in such a way. We will make the distinction between the environment as seen by an external observer and the environment observed by the organism.

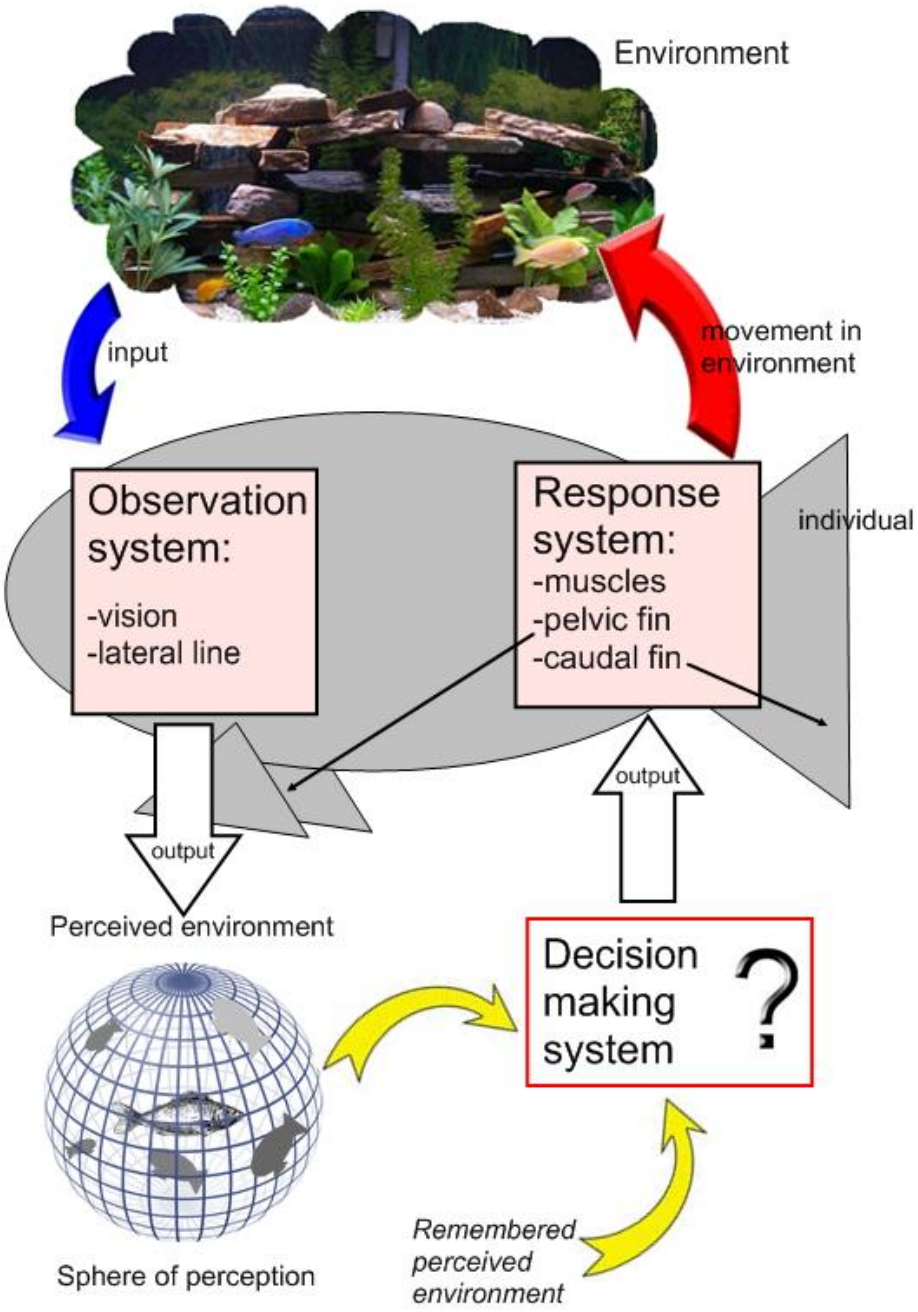

Figure 2.1: modelling framework

2.1.2 Observation system

The behaviour of an organism can only be determined by the physical interactions between the environment and the organism. The observation system enables an *active* modification of the organism's behaviour based on a particular

decision making, while for example water currents causes *passive* modifications in the movement. The extent to which the organism is capable of observing the state of the environment it is in, depends on the species. For example, various bacteria like *E. coli* and *Bacillus subtilis* are capable of measuring the concentration of particular chemical compounds in their environment through receptor molecules in their cell membrane. Receptors are protein molecules to which signaling molecules can bind. In reaction to changes in the environment, the receptor can change its shape, which will cause a cellular response. Chemical reactions involving compounds like these are a first step in a chain of so-called response regulators and secondary messenger molecules. The state of the environment, i.e. the outside total concentration of molecules, is thus encoded in an internal level of (a) messenger molecule(s).
Since these bacteria are $\sim 1\mu m$ long, they are not able to determine whether there is a higher concentration of a compound on the front or back side. They may use a kind of memory in the form of internal biochemical signals to compare the concentration in their environment to the concentration a moment before. If the concentration decreases, it will 'decide' to change direction and to move in another, random, direction (the so-called 'run-and-tumble' movement). The biophysical and biochemical details of the receptor, the response regulator and the secondary signaling molecules and how these influence the molecular motors that drive the bacterial movement can and have been studied extensively.
For *E. coli*, the output of the observation system is a particular (combination

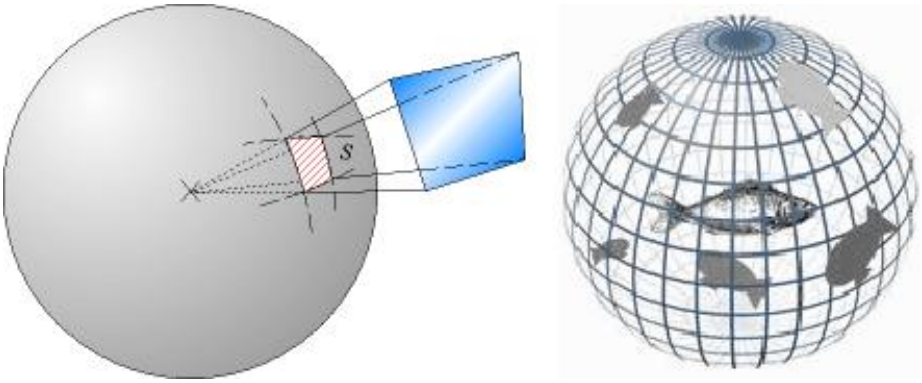

Figure 2.2: Observation of surrounding by fish.

of) internal signaling molecule(s). It is commonly accepted that there cannot be directional information in this signal. In case of vision and lateral line in fish, the output is essentially particular neural activity of the retina and lateral line. There is directional information in this signal. We view this internal signal (in both cases, i.e. with and without spatial information) as represented by a function, or more general, a measure on the sphere S^2 in three dimensions, which represents all directions. We call this the *sphere of perception* of the environment.
For example for fish, there are two situations possible. In the first situation all neighbours are spread apart and hence produce distinct spots on the sphere of perception, possibly with different (light) intensity, see Figure 2.2. In the second situation, fish can be hidden behind each other, which produces overlapping

images of neighbours on the sphere. In the first situation, the method of Couzin can be partially justified as we will show in Section 4.1, but the second case is different. It seems that it has not been considered in the literature so far.

2.1.3 Response system

How fish will respond to their environment depends on the state they are in, e.g. foraging, and the type of model used. On the discrete decision moments, the observed environment will be converted into a physical response. Very intense, dark, spots will most likely lead to repulsion, medium intense spots to alignment and spots with low intensity to attraction. By storing all the information on the same sphere, it is also possible to combine the aggregation rules from the different zones. It is likely that fish want to avoid collision by turning away from their neighbours, but still remain close to the school and keep the same direction as most of its neighbours.
We will investigate two models; one with constant speed, followed by a variable speed model. In the first model, the response only determines which way the fish will turn to in the next time step, whereas in the second model the speed can also be adjusted, which is more realistic. Our assumptions on this part are based on the predicted energy expenditure in different states. The more energy an organism wants to invest in its movement, the larger the acceleration or turning angle will be. We will investigate the response of fish in more detail in the next chapters.

2.1.4 Decision making system

Neighbours produce spots on the sphere of perception which may vary in intensity. The intensity depends on factors such as the distance, water quality, depth, lighting, time of the day, etc. On discrete decision moments, the organisms decide what to do with the information stored on their sphere of perception. How this works internally is obviously hard to investigate experimentally. Nevertheless, this part of our framework is very important. We will clarify the importance of the decision making system in Section 2.2.

2.2 Mathematical model

We shall now describe how the framework of observation, decision making and response is used in our high-level mathematical model. This model is formulated in discrete time where each time step corresponds with $\Delta\tau$ of physical time.

At every time step t, the environment $\mathcal{E}_t$ exists of:

- The position of every individual fish;
- Its orientation;
- Sea properties such as water level, depth, sea floor conditions, obstacles, predators, ...;

- Lighting conditions,

Every fish i observes the environment with its observation system, resulting in an observed environment ε_t^i. This observed environment is considered a finite measure on the sphere of perception: $\varepsilon_t^i \in \mathcal{M}(S^2)$.
We introduce the map O:

$$\begin{aligned} \mathcal{E}_t &\overset{O_i}{\to} \varepsilon_t^i \\ \mathcal{E}_t &\overset{O}{\to} (\varepsilon_t^1, \varepsilon_t^2, \cdots, \varepsilon_t^N). \end{aligned}$$

with N the number of fish in the environment.

As shown in Figure 2.1, the observed environment is mapped to the response system. We consider this map as consisting of two subsequent steps. Firstly, from the observed environment a desired direction for movement is obtained. We view this intermediary output as a *probability measure* μ on S^2, the set of possible directions. Thus, we allow stochastics in the decision making, which is reasonable in view of the poor experimental accessibility and possible biophysical complexity of this process. Secondly, for each desired direction d_i' there corresponds a setting σ of steering and propulsion parameters.
Let

$$\begin{aligned} \Psi &: S^2 \to \Sigma \\ &\quad d_i' \mapsto \sigma \end{aligned}$$

Thus we have two maps:

$$\begin{aligned} D_1 : \mathcal{M}(S^2) \to \mathcal{P}(S^2) &: \varepsilon_t^i \mapsto \mu_t^i, \\ D_2 : \mathcal{P}(S^2) \to \mathcal{P}(\Sigma) &: \mu_t^i \mapsto \mu_t^i \circ \Psi^{-1}. \end{aligned}$$

For each setting σ of steering parameters, the fish will change its spatial position in the physical time interval $[t(\Delta\tau), (t+1)(\Delta\tau)]$ according to a trajectory determined by Newtonian mechanics. This trajectory is a solution to the equations of motion:

$$\begin{cases} \dot{x}(t) = v(t), & x(0) = x^i \in \mathbb{R}^3, \\ \dot{v}(t), = F(x(t), v(t), \sigma) & v(0) = v^i \in \mathbb{R}^3, \end{cases} \tag{2.2.1}$$

where $F : (\mathbb{R}^6 \times \Sigma) \to \mathbb{R}^3$ is suitably smooth, such that the system can be solved on the interval $[0, \Delta\tau]$ yielding the operator

$$\Phi_\tau^\sigma : \mathbb{R}^6 \to \mathbb{R}^6$$

Now for $\tau \in [0, \Delta\tau]$, $\tau \mapsto \Phi_\tau^\sigma(x^i, v^i)$ determines the trajectory of the individual fish in the interval $[0, \Delta\tau]$. We define our position and velocity in the next time step as:

$$(x_{t+1}^i, v_{t+1}^i) := \Phi_{\Delta\tau}^{\sigma^i}(x_t^i, v_t^i)$$

We can extend Φ_τ^σ trivially to a map

$$\begin{aligned} \hat{\Phi}_\tau : \mathbb{R}^6 \times \mathcal{M}(S^2) \times \Sigma &\to \mathbb{R}^6 \times \mathcal{M}(S^2) \times \Sigma \\ (x, v, \varepsilon, \sigma) &\mapsto (\Phi_\tau^\sigma(x, v), \varepsilon, \sigma) \end{aligned}$$

Hence there exists a deterministic semi-flow $(\hat{\Phi}_\tau)_{\tau\in[0,\Delta\tau]}$ in the state space of each individual fish, $\mathbb{R}^6 \times \mathcal{M}(S^2) \times \Sigma$.

Thus, our model is a *randomly switched system*, where switching occurs at deterministic moments, namely at $\Delta\tau, 2\Delta\tau, \cdots$, while the stochasticity resides solely in the decision making system: at switching times a new parameter σ is selected from a distribution (law) determined through $D = D_2 \circ D_1$ from the observed environment. Thus, two fish with exactly the same observed environment, might still respond slightly different. We can view this as a "switched system", since we are alternating the deterministic dynamics with (biased) stochastic jumps in $\mathcal{M}(S^2) \times \Sigma$-space.
So concluding, the dynamics of our switched system consist of the iteration of the position, velocity, observed environment and steering parameters. This can be described in four steps:

$$(x_t^i, v_t^i, \varepsilon_t^i, \sigma_t^i)_{i=1}^N$$

$$\overset{(1)}{\downarrow}$$

by evolving these parameters over the interval $[0, \Delta\tau]$ via $(\hat{\Phi}_\tau)_{\tau\in[0,\Delta\tau]}$ for every fish, independent of one another

$$\mathcal{E}_{t+1} = (\hat{x}_{\Delta\tau}^i, \hat{v}_{\Delta\tau}^i, \varepsilon_{\Delta\tau}^i, \sigma_{\Delta t}^i)_{i=1}^N$$

$$\overset{(2)}{\downarrow}$$

where $\hat{x}_{\Delta\tau}^i$ and $\hat{v}_{\Delta\tau}^i$ are solutions to (2.2.1) with initial condition x_t^i, v_t^i, via observation map O

$$\varepsilon_{t+1}^i$$

$$\overset{(3)}{\downarrow}$$

via random variable D_1

$$\mu_{t+1}^i$$

$$\overset{(4)}{\downarrow}$$

via random variable D_2

$$\sigma_{t+1}^i$$

$$\downarrow$$

$$(x_{t+1}^i, v_{t+1}^i, \varepsilon_{t+1}^i, \sigma_{t+1}^i)$$

and back to (1) again for the next step. Here (1) and (2) are deterministic and (3) and (4) are stochastic.
Hence, for every $\varepsilon_t^i \in \mathcal{M}(S^2)$ we have a random variable $D = D(\varepsilon_t^i)$ with values in S^2: the 'desired direction' corresponding to observation ε_t^i. The 'law' of this random variable is the probability measure $D_1(\varepsilon_t^i) = \mu_t^i$ on S^2, i.e. the distribution of the output on S^2 at observation ε_t^i. This results in the distribution $D_2D_1(\varepsilon_t^i)$ of σ_t^i on Σ.
The abstract analysis of the composition of $\Phi_{\Delta\tau}, O, D_1, D_2$ for all the fish together seems quite complicated, even when D is deterministic. That is why we explore these dynamics by using simulation.

2.3 Simulation

We have written a program in MATLAB to simulate the movement of fish which implements the framework of separating observation, decision making and response. This framework is recognisable in the MATLAB program. In the appendix one can find the pseudo code, which only describes the global structure of the program which is based on our framework. With this model, one can easily adapt the different constituents to the organism investigated. We have made two models: one with a constant speed and one with a variable speed. These models will be explained in the Chapters 4 and 5.

2.3.1 Implementation of sphere of perception

The output of the observation system is represented as a density function or measure over the sphere S^2 of directions. This function is in turn represented in spherical coordinates. Before we can convert the Cartesian coordinates of every neighbour fish observed by fish i into spherical coordinates, we first have to transform the Cartesian coordinates in such a way that the direction vector of fish i is placed on the x-axis. This is done by two rotations, produced by two rotation matrices. We assume that the horizontal angle of the direction vector of fish i, ϑ, and the vertical angle of this direction vector, φ, both measured from the positive x-axis, are positive, so by first rotation clockwise horizontally and than clockwise vertically, we find that our new positions in Cartesian coordinates are given by

$$\begin{bmatrix} x' \\ y' \\ z' \end{bmatrix} = \begin{bmatrix} \cos(\varphi) & 0 & \sin(\varphi) \\ 0 & 1 & 0 \\ -\sin(\varphi) & 0 & \cos(\varphi) \end{bmatrix} \begin{bmatrix} \cos(\vartheta) & \sin(\vartheta) & 0 \\ -\sin(\vartheta) & \cos(\vartheta) & 0 \\ 0 & 0 & 1 \end{bmatrix} \begin{bmatrix} x \\ y \\ z \end{bmatrix}$$

so we find that

$$\begin{bmatrix} x' \\ y' \\ z' \end{bmatrix} = \begin{bmatrix} \cos(\varphi)\cos(\vartheta) & \cos(\varphi)\sin(\vartheta) & \sin(\varphi) \\ -\sin(\vartheta) & \cos(\vartheta) & 0 \\ -\sin(\varphi)\cos(\vartheta) & \sin(\varphi)\sin(\vartheta) & \cos(\varphi) \end{bmatrix} \begin{bmatrix} x \\ y \\ z \end{bmatrix}.$$

The Cartesian coordinates of every neighbour of fish i are now converted to spherical coordinates where we use the conventions employed by MATLAB. That is, we express the position of each fish in three variables: the radial distance r of fish j from fish i, its elevation angle φ measured from the direction of fish i, and the azimuth angle ϑ of its orthogonal projection on a reference plane that passes through the origin and is orthogonal to the zenith, measured from the direction of fish i on that plane, see Figure 2.3.
In Figure 2.3, $\varphi \in [-\frac{1}{2}\pi, \frac{1}{2}\pi]$ and $\vartheta \in [-\pi, \pi)$. Note that the literature is not consequent on this part: some authors use another spherical representation where $\varphi \in [0, \pi]$ is the inclination angle measured from the positive z-axis.
Now we divide ϑ and φ in regions of size $\frac{\pi}{M}$, where M is a positive integer. This divides our surface into boxes which can be represented by a matrix of size $2M \times M$, so every box has a row and a column number. This way we are able to store in which box there is (part of) a neighbour spotted by fish i and how intense this spot is. This intensity can be measured in two parts: the first part

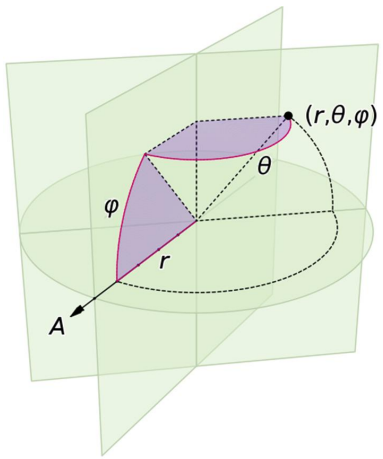

Figure 2.3: Spherical coordinates in MATLAB (by Jorge Stolfi

is created by the vision and is a function of the distance to the neighbour, its length and its thickness; the second part is created by the lateral line which also uses the direction of the neighbouring fish.
The observed length of a neighbouring fish j seen from fish i is given by $L' = L \sin\gamma$, see Figure 2.4. If we only consider the length of fish j, this describes an angle ς on the sphere of perception:

$$\varsigma \approx \frac{L'}{2\pi|\vec{c_j} - \vec{c_i}|} \tag{2.3.1}$$

where $\vec{c_j} - \vec{c_i}$ represents the vector from fish i to the centre of fish j, $\vec{d}$ the direction of fish i, see Figure 2.4. Hence the further away a neighbour is, the smaller the region occupied on the sphere of perception and the larger a neighbour, the larger this region is.
We also want to incorporate the thickness of the fish into the intensity function. This way a neighbour swimming in the viewing direction of fish i does not produce one single point, but a larger spot. The thickness of the fish remains the same, since we consider our fish to be approximately cylindrical.

If a box is already occupied when another neighbour is localised at the same box, only the one with the smallest (absolute) distance will be stored in this box. This way (part of) fish hidden behind (part of) others will not be seen by or influence the decision of fish i.

Since we make the distinction between information collected from vision and the lateral line, we can combine these in the region of repulsion and alignment where both are used. In the attraction zone, only vision is used. Fish have different blind zones for vision and for the lateral line, [9], which explains why some boxes of our observation matrix will not be filled. In Figure 2.5 it is pointed out which boxes can store which kind of information. Here one can exclude the top and bottom row, since it might be impossible for fish to see straight above and below them.
Another purpose for which this observation system can be used, is to detect

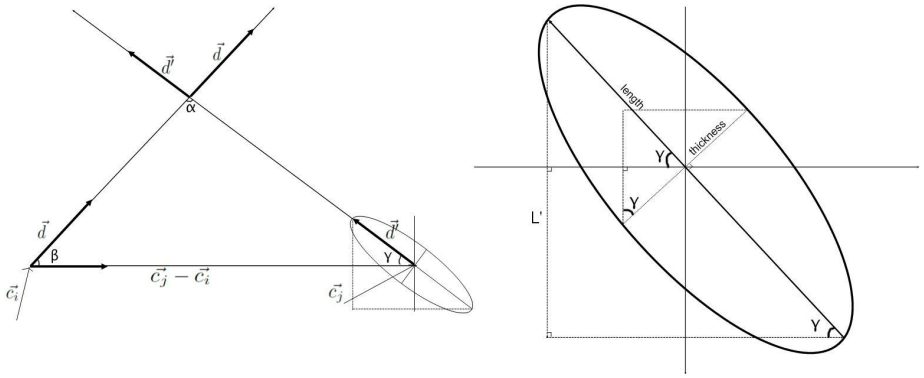

Figure 2.4:

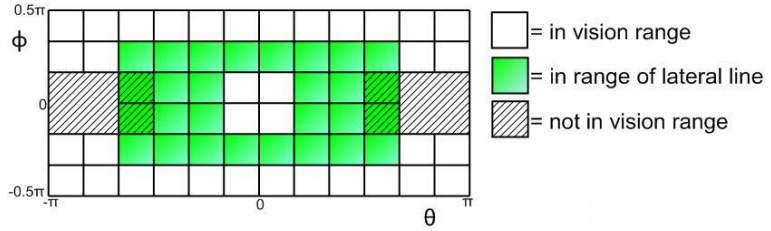

Figure 2.5: Storing observation information in boxes

other objects and species, for example predators and food. Since fish have a high priority to avoid predators, it is a possibility to give predators negative values, which will cause a different response from our individual fish. The same can be done for food, but then in a attracting way. Depending on the state a fish is in, it will prefer to feed or stay close to a school and hence respond differently to an equal environment in a different state.

Triangulation of the fish

We use triangles to present neighbouring fish and the spots they produce on the sphere of perception. This is a common method, since this is the smallest surface possible and by using triangles, all surfaces, or bodies, can be very well approximated. We used a single triangle per fish in our implementation to prove our concept. This can be extended in a way such that the spot has the shape of a fish. It can even be used to build in skin patterns or colors, which may have different influences on the fish; by making the head of a fish a different color, this might reflect the light more which causes the fish to be more attracted by its neighbours head than its tail, which might result in more alignment.
In our simulation we use the three points defining the triangle and connecting them by a straight line in the matrix representing the sphere of perception, and filling the boxes in between. We had to be careful at this point, when a neighbouring fish is located straight above or below the observing fish, this will result in a spot covering (at least) one entire row, so connecting the three

points does not suffice in this case. Hence we have to check if the solid triangle generated by the three point, A, B, C, intersect the z-axis, $\mathbb{R}e_z$. To that end, consider $X = [\vec{x_A}, \vec{x_B}, \vec{x_C}]$, the matrix containing three vectors point towards A, B and C. These vectors span a convex cone.

Proposition 1. *The solid triangle generated by the vectors $\vec{x_A}, \vec{x_B}, \vec{x_C}$ in $\mathbb{R}^3$ intersects the z-axis, i.e., conv$(\{\vec{x_A}, \vec{x_B}, \vec{x_C}\}) \cap \mathbb{R}e_z \neq \emptyset$, if and only if*
(i) $\det(X) \neq 0$ *and sign*$(\det(X_i))$=*sign*$(\det(X_j))$ *whenever* $\det(X_i) \neq 0$ *and* $\det(X_j) \neq 0$*, or*
(ii) $\det(X) = 0$ *and* $\det(X_i) = 0\ \forall i$.

Proof. "⇒": There exists $\lambda_i \in [0,1] : \sum_i \lambda_i = 1$ and $\mu \in \mathbb{R}^3$ such that

$$\lambda_1 \vec{x}_A + \lambda_2 \vec{x}_B + \lambda_3 \vec{x}_C = \mu e_z. \tag{2.3.2}$$

In particular, $X\hat{\lambda} = e_z$ has a solution $\hat{\lambda}$ with all entries either positive or negative.
If $\det X \neq 0$, then by Cramer's Rule we find that

$$\hat{\lambda}_i = \frac{\det(X_i)}{\det(X)}, \tag{2.3.3}$$

where X_i is the matrix X with the i-the column replaced by the vector e_z. Then the $\det(X_i)$ must have the same sign when non-zero.
If $\det(X) = 0$, the three vectors $\vec{x_A}, \vec{x_B}, \vec{x_C}$ are linearly dependent. If (2.3.2) holds, then e_z and either pair of $\vec{x_A}, \vec{x_B}$ and $\vec{x_C}$ is linearly dependent, i.e. $\det(X_1) = \det(X_2) = \det(X_3) = 0$.
"⇐": Consider the equation $X\hat{\lambda} = e_z$. If $\det(X) \neq 0$ and all $\det(X_i)$ that are non-zero have the same sign,

$$\lambda := \frac{\hat{\lambda}}{\sum_i \hat{\lambda}_i}; \tag{2.3.4}$$

$$\mu := \sum_i \hat{\lambda}_i \tag{2.3.5}$$

will satisfy (2.3.2) and $\lambda_i \in [0,1], \sum_i \lambda_i = 1$. Thus $\text{conv}(\{\vec{x_A}, \vec{x_B}, \vec{x_C}\}) \cap \mathbb{R}e_z \neq \emptyset$.
If $\det(X) = 0$, then $\vec{x_A}, \vec{x_B}$ and $\vec{x_C}$ are linearly dependent. $\text{conv}(\{\vec{x_A}, \vec{x_B}, \vec{x_C}\})$ therefore lies in a plane or line through the origin;
$\text{span}\{\vec{x_A}, \vec{x_B}, \vec{x_C}\} = \mathbb{R}e_z \cap \text{conv}(\{\vec{x_A}, \vec{x_B}, \vec{x_C}\}) \neq \emptyset$ iff $\vec{x_A}, \vec{x_B}, \vec{x_C}$ and e_z are linearly dependent. In particular, $\det(X_1) = \det(X_2) = \det(X_3) = 0$. □

If the components of λ are all positive, this means the spot is at the north pole. If all components are negative, the spot is at the south pole. In all other cases, A, B and C are not located around a pole.

2.3.2 Interpretation of sphere of perception

After the implementation of the sphere of perception, we need to use it to determine what the fish will do in the next time step in the simulation. This is

part of the decision making system of an organism, which is hard to investigate experimentally.
Before, we used the zones of repulsion, alignment and attraction in which different aggregation rules hold. By introducing the sphere of perception, we do not want to lose this concept. Since on this sphere, the intensity of the spot the neighbours produce has also been taken into account, we can use this to determine which spots will result in repulsion, alignment or attraction. A very black spot means a very close neighbour, which will make fish i turn away from this neighbour. Therefore more intense spots have higher priority than spots with low intensity. Since the intensity is a function of the distance from fish i to its neighbours, we can use this to determine which spots result in which type of aggregation. This way it is also possible to combine the different zones.
In Section 3.1 we will show how the intensity of the spots can be used to determine the sizes of the different aggregation zones. We will describe in Section 4.1 how the sphere of perception can be used to determine the desired direction for the next time step.

Chapter 3

Some physics of fish vision and swimming

In this chapter we will investigate the physics and the visual system of fish in more detail. We will provide an improvement to the models used by previous researchers on the part where the absolute distance to neighbours is used, by introducing a *perceived distance* in the next section. In Section 3.2 and 3.3 we will investigate how the speed of a fish will change by taking into account the amount of power investigated in swimming by a fish. We will investigate how turning effects the speed, when a fish stops investing energy in its movement.

3.1 Characteristics of the visual system

Vision plays an important role in schooling behaviour. Fish spot their neighbouring fish by the reflected sunlight that strikes their eye. Here we assume that the amount of reflected light is equal for all fish, despite their dept, and that the reflected light on a neighbouring fish has an effective radiant power p. That is, the differential sensitivity of the fish eye to various wave lengths and differences in the reflectiveness of the fish for the wave lengths is expressed as the total amount of energy per unit of time and per unit area, that is reflected by the neighbouring fish as can be observed by the fish eye.
The amount of light reflected by a neighbouring fish depends on the light intensity. The intensity is a measure for the energy flux density, i.e. if $\mathcal{S}$ is some surface and I the intensity vector, then the amount of energy flowing through the surface $\mathcal{S}$ per unit of time is equal to

$$P_{\mathcal{S}} = \int_{\mathcal{S}} I \cdot dA.$$

If there is no energy loss to the medium, in this case water, the intensity will decrease in proportion to the squared of the distance to the source. If the surface $\mathcal{S}$ is a sphere of radius r centred at the light point source, conservation of energy

yields

$$P = |I| \cdot 4\pi r^2, \tag{3.1.1}$$

where P is the radiant power of the source.
In any medium, light energy is absorbed at exponential rate, depending on the wavelength, which is commonly called attenuation. Now equation (3.1.1) becomes

$$e^{-\alpha r} P = |I| \cdot 4\pi r^2,$$

where α is the attenuation rate or absorption coefficient which depends on the wave length and the medium the light is travelling through.
Now we find for a point source with radiant power P

$$|I| = \frac{P}{4\pi r^2 e^{\alpha r}}.$$

The light energy striking the fish eye surface $\mathcal{S}_{eye}$ of area $\mathcal{A}_{eye}$ reflected by the neighbouring fish surface $\mathcal{S}_{fish}$ equals

$$\begin{aligned} P_{eye} &= \int_{\mathcal{S}_{eye}} I^{tot} dA \\ &= \int_{\mathcal{S}_{eye}} \left(\int_{\mathcal{S}_{fish}} \frac{p(r)}{4\pi r^2 e^{\alpha r}} \frac{\vec{r}}{|\vec{r}|} d\mathcal{S} \right) dA \\ &\approx \mathcal{A}_{eye} \int_{\mathcal{S}_{fish}} \frac{p(r)}{4\pi r^2 e^{\alpha r}} d\mathcal{S} \end{aligned} \tag{3.1.2}$$

where p is the radiant power density distribution over the fish skin surface. For simplicity, we assume $p(r) \equiv \bar{p}$, so we find

$$P_{eye} \approx \mathcal{A}_{eye} \frac{\bar{p} \mathcal{A}^{eff}_{fish}}{4\pi \bar{r}^2 e^{\alpha \bar{r}}}$$

where $\mathcal{A}^{eff}_{fish}$ is the surface area that is effectively visible and $\bar{r}$ the distance to the centre of mass of the neighbouring fish. Note that $\mathcal{A}^{eff}_{fish}$ depends on $\mathcal{A}_{fish}$ and the longitudinal swimming direction of this neighbouring fish. Recall from Section 2.3.1 that the effective visible surface area is given by $\mathcal{A}_{fish} \sin(\gamma)$.
The height of a fish is related to its length: $h = c \cdot BL$. For the capelin $h \approx \frac{1}{7} BL$, see Figure 3.1.

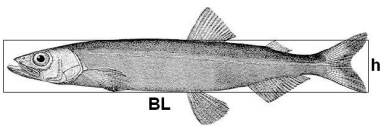

Figure 3.1: Height to body length ratio for the capelin

Hence we can write $\mathcal{A}_{fish} = c_0 \cdot hBL = c_1 BL^2$ where c_1 depends of the shape

of the fish and the proportion of the length and height of the fish.
Now we find that we can approximate the radiant power in the eye by

$$\begin{aligned} P_{eye} &= \frac{\bar{p}c_1\mathcal{A}_{eye}\sin(\gamma)}{4\pi}\frac{BL^2}{r^2}e^{-\alpha r} \\ &= C\left(\frac{BL}{r}\right)^2 e^{-\alpha r} \end{aligned}$$

If we assume that the fish eye is sensitive to signals above a total power P^0_{eye}, then we obtain a natural bound r^* for vision:

$$C\left(\frac{BL}{r^*}\right)^2 e^{-\alpha r^*} \geq P^0_{eye}$$

By assuming the ideal situation, we can neglect attenuation, hence $\alpha = 0$ and we obtain

$$\frac{BL}{r^*} \geq \sqrt{\frac{P^0_{eye}}{C}}$$

hence

$$\frac{r^*}{BL} \leq \sqrt{\frac{C}{P^0_{eye}}} \tag{3.1.3}$$

$$= \sqrt{\frac{\bar{p}c_1\mathcal{A}_{eye}\sin(\gamma)}{4\pi P^0_{eye}}} \tag{3.1.4}$$

We can conclude that the maximal radius of the visual system for effective detection of other fish, expressed in body length, depends rather simply on the shape of the fish, skin structure and properties of the fish eye itself, according to equation (3.1.4).
For the lateral line, we might be able to determine a maximal radius in a similar way. These constraints lead to the sizes of the different aggregation zones: the zone of repulsion, alignment and attraction.

3.2 Energy and power expenditure

One of the main reasons for fish to school, is to save energy. Here we will investigate the total energy expenditure per time unit, the power, of an organism seen as rigid body subject to Newtonian mechanics, in order to make predictions about the speed of fish in different states.
The total power needed for movements depends on different aspects like the metabolic power (for heartbeat, create nutrients for muscles, etc), velocity and acceleration. Hence the effective power is smaller than the total power invested by the organism. The latter we cannot measure, but we can investigate the power needed for locomotion. Swimming involves the transfer of momentum from the fish to the surrounding water en vice versa, where the main momentum transfer mechanisms are via drag lift and acceleration. Swimming drag consists of three components:

- Skin friction between the fish and the boundary layer of water (*viscous or friction drag*);
- Pressure formed in pushing water aside for the fish to pass (*form drag*);
- Energy lost in the vortices formed by fins to generate lift and thrust (*vortex or induced drag*).

The latter two components are jointly described as *pressure drag* [18].
According to Sparenberg and Lighthill [19], the rate of shedding kinetic energy into the water when fish are swimming in a straight line can be approximated by:

$$P^{loss} \approx \frac{1}{2}C|v(t)|^3 \tag{3.2.1}$$

where C depends on parameters like the drag coefficient, the size of the fish and the water density. We found a similar approach by Videler [21] that is further developed in [6]. While swimming, fish experience drag from the water. In order to move through the water, the power needed to cancel the drag onto the fish is called the thrust. While steering, fish also lose energy. Since the kinetic energy is given by $E_{kin} = \frac{1}{2}m|v|^2$ we can write the change in kinetic energy as

$$\begin{aligned} \frac{dE_{kin}}{dt}(t) = mv(t)\cdot\frac{dv}{dt} &= P_t^{thrust} - [P^{drag}(v_t) + P^{steering}(v_t,\dot{\theta})] \\ &= P_t^{thrust} - P_t^{loss} \end{aligned} \tag{3.2.2}$$

where $P^{loss} \geq 0$ and $\dot{\theta}$ is the angular velocity of the reorientation movement which is a function of the angle θ that the caudal fin makes with respect to the longitudinal direction of the fish. Here we do not consider the total power invested by the fish, since this also includes the metabolic power. How this power is used internally, which muscles are used and how, has been investigated thoroughly, but will not be discussed here. We refer interested readers to [5, 21].
We first look at the case when the fish decides to stop investing energy into its movement. Hence $P^{thrust} = P^{steering} = 0$, but we assume that the speed at this moment is positive. The remaining equation is

$$\frac{dE_{kin}}{dt} = -\frac{1}{2}C|v(t)|^3. \tag{3.2.3}$$

By substituting $y = \frac{2E_{kin}}{m} = |v|^2$, (3.2.3) reduces to

$$\frac{dy}{dt} = -\frac{C}{m}|y|^{3/2}. \tag{3.2.4}$$

with $y(0) = y_0 > 0$.

We can solve this differential equation by separation of variables to find

$$y(t) = \frac{1}{(\frac{C}{2m}t + \frac{1}{\sqrt{y_0}})^2}. \tag{3.2.5}$$

Notice here that for all $t \geq 0, y(t) > 0$, so $v^2 > 0$ and hence the fish will keep moving. This is in an ideal situation where the water is completely still, which is not very realistic. To overcome this problem, one can introduce a threshold for the speed; if the speed drops below this threshold, the speed is considered to be equal to zero.

3.3 Horizontal steering

Many fish use their tail fin, or caudal fin, as the main propulsive and horizontal steering device [21][1]. The amount of flexibility of the caudal fin depends on the type of fish and the type of swimming required to optimize survival. For slow-swimmers, manoeuvrability is more important than the ability to generate large propulsive forces, whereas for pelagic fish it is the other way around. In [5,21] the authors describe in detail how the different muscles work in both types of fish. Beside the caudal fin, other fins may take part in steering and propulsion, depending on the type of fish.
Here we will investigate how the steering power is related to the movement of the caudal fin. We will therefore consider neutrally buoyant fish which mainly use their tail fin for thrust and horizontal steering.
From a physical point of view, we look at the fish as a rigid body. According to [5, p.84] fast swimmers like tuna can be very well described by a more of less rigid body to which a caudal oscillating propeller is attached. There they describe two methods to analyse the process of generating forward thrust: by a lift-based or vorticity approach, or by a bulk momentum or added mass method.

3.3.1 Turning angle as function of tail angle

When a fish wants to change its direction, it will bend its tail fin to generate an extra drag force which will make the fish both slow down and turn, see Figure 3.2A. This additional drag force creates a momentum $\vec{M}$ with respect to the centre of mass: the tendency of a force to rotate an object about an axis. To calculate $\vec{M}$, we need the moment arm $\vec{r}$ which is the vector from the centre of mass R to the point where the net force $\vec{F}_{tail}$ is working on the tail fin. The distance of the centre of mass to the starting point of the tail P is designated by l. The distance from P to the point where the force is working on is d. The force working on the tail fin is pointing in the swimming direction of the fish.
Now

$$\begin{aligned} \vec{M} &= \vec{r} \times \vec{F}_{tail}, \\ M &= rF_{tail} \sin(\phi), \end{aligned}$$

with $M = |\vec{M}|, r = |\vec{r}|, F = |\vec{F}|$ and ϕ is the angle between the mid line of the fish and $\vec{r}$.
Let θ be the angle between the tail fin and the main body of the fish, as shown in Figure 3.2A. We know that $F_{tail} = \frac{1}{2} C' A_{tail} |\sin(\theta)| v^2$ where $A_{tail}|\sin(\theta)|$ represents the reference area which creates the extra drag force. This reference

[1] Recall Figure 1.2 for the used terminology for fish

area depends on the size of the tail fin and the angle it is bend in; a larger tail or angle will create a larger force and hence a larger turning rate.

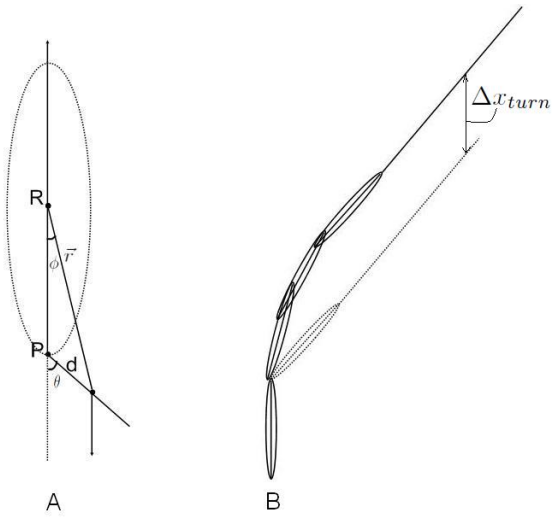

Figure 3.2: A: Turning. B: Shifting from desired direction.

Notice that $r\sin(\phi) = d\sin(\theta)$. Thus

$$\begin{aligned} M &= F_{tail} d \sin(\theta) \\ &= \frac{1}{2} C' A_{tail} d \sin(\theta) |\sin(\theta)| v^2. \end{aligned} \tag{3.3.1}$$

Now we will take a look at the angular momentum, given by

$$\vec{J} = m\vec{r} \times \dot{\vec{r}}$$

(Kibble, [13]).
Since we are interested in the horizontal rotation, we can consider the rotation about the fixed z-axis $J_z = I\omega$ where ω is the angular velocity of the rotation about the z-axis and I is the moment of inertia: this describes the resistance of an object to change its rotation rate.
In general, for a solid rigid body with mass density distribution $\rho(x)$ and the distance r of part x in the body to the centre of mass, the moment of inertia with respect to the centre of mass is given by $I = \int r^2 \rho(x) dx$.
Now let us go back to the equation $J_z = I\omega$. Differentiating both sides with respect to time gives

$$\begin{aligned} \dot{\vec{J}}_z &= m\dot{\vec{r}} \times \dot{\vec{r}} + m\vec{r} \times \ddot{\vec{r}} \\ &= 0 + m\vec{r} \times \ddot{\vec{r}} \\ &= \vec{r} \times \vec{F} = M \end{aligned}$$

since the cross product of a vector with itself is zero. Hence

$$\begin{aligned} I\dot{\omega} &= M \\ \dot{\omega} &= \frac{M}{I}. \end{aligned}$$

Now by substituting (3.3.1) we find

$$\dot{\omega} = \frac{1}{2}\frac{C'}{I}A_{tail}d\sin(\theta)|\sin(\theta)|v^2 \tag{3.3.2}$$

Since we know from the schooling rules what the desired turning angle α for a fish should be in a time step $\Delta\tau$, we now know the change of direction in one time step assuming that $\dot{\omega}$ remains approximately constant in that time interval;

$$\begin{aligned}\Delta\alpha &\approx \frac{1}{2}\dot{\omega}\Delta\tau^2 \\ &= \frac{1}{4}\frac{C'}{I}A_{tail}d\sin(\theta)|\sin(\theta)|(v\Delta\tau)^2. \end{aligned}\tag{3.3.3}$$

Since I is a constant, we would like to make a good estimate for this. We can compare our fish, the rigid body, to a thin cylinder, a rod, with the axis of rotation at the end of the rod. Then I can be estimated by $I = \frac{1}{3}mL^2$ where L is the length of the rod which corresponds to the body length, BL, of the fish. Then equation (3.3.2) and (3.3.3) become respectively

$$\begin{aligned}\dot{\omega} &= \frac{1}{2}\frac{3C'}{mBL^2}A_{tail}d\sin(\theta)|\sin(\theta)|v^2. \\ \Delta\alpha &= \frac{1}{4}\frac{3C'}{mBL^2}A_{tail}d\sin(\theta)|\sin(\theta)|(v\Delta\tau)^2. \end{aligned}\tag{3.3.4}$$

Now it follows from (3.3.4) that

$$\begin{aligned}|\sin(\theta)|^2 &= \frac{4|\Delta\alpha|mBL^2}{3C'A_{tail}d}\cdot\frac{1}{(v\Delta\tau)^2} \\ |\sin(\theta)| &= 2BL\sqrt{\frac{m}{3C'A_{tail}d}}\cdot\frac{\sqrt{|\Delta\alpha|}}{|v\Delta\tau|}. \end{aligned}$$

Now we notice that the additional loss in kinetic energy per unit of time due to horizontal steering equals approximately

$$\begin{aligned}F_{tail}v &= \frac{1}{2}C'A_{tail}|\sin(\theta)|v^3 \\ &= BL\sqrt{\frac{C'A_{tail}m}{3d}}\cdot\frac{\sqrt{|\Delta\alpha|}v^2}{\Delta\tau}. \end{aligned}$$

From this last equation and equation (3.2.2) we are able to give an educated guess for the new velocity at the next time step, given we know how much power a fish wants to invest in its situation. This will be investigated in Section 5.3. From the last equation we are also able to determine the maximal angle possible to turn in one time step. Therefore we need to know how flexible the tail of a specific fish type is. This information is incorporated in the fish-dependent constant C'. Then we know θ and hence we can calculate how much a fish can change its direction in $\Delta\tau$. Since $\sin(\theta) \leq 1$, we know that

$$\begin{aligned}\Delta\alpha &\leq \frac{1}{4}\frac{C'}{I}A_{tail}d(v\Delta\tau)^2 \\ \alpha_{max} &= \frac{1}{4}\frac{C'}{I}A_{tail}d(v\Delta\tau)^2. \end{aligned}$$

3.3.2 Loss of speed due to turning

In the previous section we calculated how much a fish can turn in one time step and how the speed changes if a fish stops investing energy in swimming. By turning, the speed of a fish reduces even more. We can investigate this by adding a total steering component $\tilde{C}\frac{\sqrt{|\Delta\alpha|}v^2}{|\Delta t|}$ where $\tilde{C} = BL\sqrt{\frac{C'A_{tail}m}{3d}}$ to equation (3.2.3) and (3.2.4) in order to get

$$\begin{aligned} \frac{dE_{kin}}{dt} &= -\frac{1}{2}C|v(t)|^3 - \tilde{C}\frac{\sqrt{|\Delta\alpha|}v^2}{|\Delta\tau|} \\ \frac{dy}{dt} &= -\frac{C}{m}|y|^{3/2} - \frac{2\tilde{C}}{m}\frac{\sqrt{|\Delta\alpha|}}{|\Delta\tau|}y. \end{aligned} \tag{3.3.5}$$

where $y = \frac{2E_{kin}}{m} = v^2$. By taking $a = \frac{C}{m}, b = \frac{2\tilde{C}}{m}\frac{\sqrt{|\Delta\alpha|}}{|\Delta t|}$, (3.3.5) becomes

$$\begin{aligned} \frac{dy}{dt} &= -(ay^{3/2} + by) \\ \int \frac{1}{ay^{3/2} + by}dy &= -t \\ \int \frac{1}{2\sqrt{y}}\frac{1}{\frac{a}{2}y + \frac{b}{2}\sqrt{y}}dy &= -t \end{aligned}$$

By substituting $z = \sqrt{y}, dz = \frac{1}{2\sqrt{y}}$ we find

$$\begin{aligned} \int \frac{1}{\frac{a}{2}z^2 + \frac{b}{2}z}dz &= -t \\ \int \frac{1}{z}\frac{1}{\frac{a}{2}z + \frac{b}{2}}dz &= -t \end{aligned}$$

and by using partial fraction we get

$$\begin{aligned} -t &= \int \frac{\frac{2}{b}}{z} - \frac{\frac{a}{b}}{\frac{a}{2}z + \frac{b}{2}}dz \\ &= \frac{2}{b}\ln|z| - \frac{2}{b}\ln\left|\frac{a}{2}z + \frac{b}{2}\right| + C_0 \\ &= \frac{2}{b}\left(\ln|z| - \ln\left|\frac{a}{2}z + \frac{b}{2}\right|\right) + C_0 \\ &= \frac{2}{b}\left(\ln z - \ln\left(\frac{a}{2}z + \frac{b}{2}\right)\right) + C_0 \\ &= \frac{2}{b}\left(\ln z - \ln\left(\frac{1}{2}(az + b)\right)\right) + C_0 \\ &= \frac{2}{b}\ln\left|\frac{2z}{az + b}\right| + C_0 \\ &= \frac{2}{b}\ln\left|\frac{2v}{av + b}\right| + C_0 \end{aligned}$$

where $C_0 \in \mathbb{R}$. Now we find that

$$\begin{aligned} \ln\left(\frac{2v}{av+b}\right) &= -\frac{b}{2}t - \frac{bC_0}{2}, \\ \frac{2v}{av+b} &= C_0' e^{-\frac{b}{2}t}, \end{aligned}$$

from which we find

$$v = \frac{bC_0' e^{-\frac{b}{2}t}}{2 - aC_0' e^{-\frac{b}{2}t}}.$$

Since b is a function of the turning angle, we have now expressed the new speed in the angle turned, which in turn depends on properties of the fish and the surrounding water.
In a similar way, the vertical rotation can be incorporated by using the pelvic fins instead of the caudal fin.

Translational shift in turning
While steering, fish change direction. Since they are already swimming with a certain speed $v > 0$, they tend to drift sideways while turning. This results in a shifting from the desired trajectory, see Figure 3.2B.
What does this mean for the new position of the fish? If a fish stops investing energy and does not turn, we know that the speed is given by

$$v(t) = \frac{1}{\frac{C}{2m}t + \frac{1}{v_0}},$$

and the distance travelled in one time step is given by

$$\Delta x = v_0 \int_0^{\Delta\tau} \frac{1}{v_0 \frac{C}{2m}t + 1} dt \tag{3.3.6}$$

$$= \frac{2m}{C} \ln\left(\frac{v_0 C}{2m}\Delta\tau + 1\right). \tag{3.3.7}$$

Hence we know that the translational shift $\Delta x_{turn} \leq \Delta x$ when turning.

Chapter 4

A constant speed model

We model and simulate fish in a three dimensional water tank that has periodic boundaries horizontally: fish that swim out on one side, will enter the tank again on the opposite side. At every time step, the position vector of its centre of mass c_i, and velocity vector v_i are updated for every individual. In this chapter, the speed of the fish, $s_i = ||v_i||$, remains constant. It will be made adjustable later on in Chapter 5.
Vertically, we consider two cases. In order to compare our model with Couzin's, we simulate a version which has periodic boundary condition in vertical direction too. In the second case we include vertical boundaries caused by the water surface and the sea floor. This appears to be new.

In our three dimensional model we followed the basic aggregation rules originally described by Huth and Wissel in [11] and further developed by Hemelrijk and Hildebrandt in [9], starting with the most important rule:

- Avoid collision with neighbours in a zone close to the fish;
- Align with neighbours a bit further away;
- Be attracted by neighbours at a large distance.

These three regions are assumed to be spherical.
Previous models always used the absolute distance from a fish to its neighbours to determine how fish would react to their environment. We argued above that it is improbable that fish are able to determine this distance. Instead, we introduce a *perceived distance*, pd_j, in our simulation that we will now discuss. By using the perceived distance, a large fish appears to be closer and a very small fish further away. Hence a large neighbour might have a bigger influence in the decision than a small neighbour: it is plausible that a school, which might be seen as one very large neighbour, will have a much bigger influence on a fish than a small neighbour, which happens to be closer.

4.1 Perceived distance

Consider a fish, i, that visually spots a neighbouring fish j and suppose there are no other fish present. Fish j produces a single spot on the retina of the observing fish i. The radiant power on this spot equals

$$P_j = C\left(\frac{BL}{r_j}\right)^2 e^{-\alpha r_j},$$

see Section 3.1.
This spot is represented on the sphere of perception by a spot $E_j \subset S^2$ of area $|E_j| := \int\limits_{S^2} \mathbf{1}_{E_j} d\omega$ and intensity $I_j = \frac{P_j}{|E_j|}$. Let $\omega_{E_j} := \frac{1}{|E_j|} \int\limits_{E_j} \omega d\omega$ be the centre of mass of E_j.
We assume that the decision making system (D, see Section 2.2) transforms the perceived environment as represented by an intensity function f on the sphere of directions S^2 into a desired direction $\hat{d}'$ according to

$$\begin{aligned} d' &:= \int\limits_{S^2} \omega f(\omega) d\omega \\ \hat{d}' &:= \frac{d'}{||d'||}. \end{aligned}$$

This yields for the single spot E_j

$$\begin{aligned} d' &= \int\limits_{S^2} \omega I_j \mathbf{1}_{E_j} d\omega \\ &= I_j \int\limits_{E_j} \omega d\omega \\ &= I_j |E_j| \omega_{E_j} \\ &= P_j \omega_{E_j}, \end{aligned}$$

Hence $\hat{d}' = \omega_{E_j}$.

If there are N neighbouring fish which produce non-overlapping spots $E_1, \cdots, E_N$ of homogeneous intensity $I_1, \cdots, I_N$ respectively, then

$$\begin{aligned} d' &= \int\limits_{S^2} \omega f(\omega) d\omega = \sum_{j=1}^{N} \omega I_j \mathbf{1}_{E_j} d\omega \\ &= \sum_{j=1}^{N} P_j \omega_{E_j} \\ &\approx \sum_{j=1}^{N} C\left(\frac{BL}{r_j}\right)^2 e^{-\alpha r_j} \frac{\vec{r_j}}{|\vec{r_j}|} \end{aligned}$$

where $\vec{r}_j$ is the vector from i to the centre of mass of fish j.
Now we define the *perceived distance* from fish i to its neighbour j by

$$\mathrm{pd}_j := C^{-1} \left(\frac{r_j}{BL}\right)^2 e^{\alpha r_j}$$

Then it follows that

$$\begin{aligned} d' &= \sum_{j=1}^{N} \frac{\vec{r}_j}{\mathrm{pd}_j} \\ \hat{d}' &= \frac{d'}{||d'||}, \end{aligned}$$

which is similar to Couzin's approach, but with the absolute distance replaced by the perceived distance, which takes attenuation, fish shape and size into account.
Once the desired direction is determined and the direction vector d_i' has been normalized to $\hat{d}_i'$, the positions can be updated by

$$c_i(t+1) = c_i(t) + s_i \cdot \hat{d}_i'(t+1) \cdot \Delta\tau. \tag{4.1.1}$$

The speed s_i can be taken constant over time, but different for every fish, or the same for all fish for all time.
For the variable speed model we will improve this approach by taking the observed environment into account, represented on the sphere of perception as will be described in Section 5.1.

4.2 Maximal turning angle

The physical limitation in response that is taken into account in the various modelling approaches in the literature, is a maximal angle over which a fish can turn in a single time step. If a fish wants to avoid collision with a neighbour right in front of it, it would like to make a turn of 180°. Since this is not possible in small time steps in reality, most discrete models incorporate a maximal turning angle per time step for every fish. We will follow this approach.
This maximal turning angle α_{max} depends on a maximal turning rate ω_{max} and the physical time step $\Delta\tau$ corresponding to one time step in our simulation: $\alpha_{max} = \omega_{max}\Delta\tau$. In Section 3.3 we have investigated this maximal turning angle for the variable speed model, based on the physics of fish motion in water.

The question is to find the vector of unit length in the plane in $\mathbb{R}^3$ spanned by the current direction of movement $v_i(t)$ and the desired direction for the next time step $d_i'(t+1)$ that has angle α_{max} with $v_i(t)$ and smallest angle with $d_i'(t+1)$. If the angle between the velocity at time t and the desired direction vector at time $t+1$ is larger than the maximal turning angle, $d_i(t+1)$ will be positioned in the direction of the maximal turning angle.
To calculate this new achievable desired direction of movement, let $\vec{a}$ the velocity vector at time t and $\vec{b}$ the desired velocity vector at time $t+1$. The achievable direction vector $\vec{x}^*$ that takes the maximal turning angle α_{max} into account is precisely the normalisation to unit length of the vector among the convex

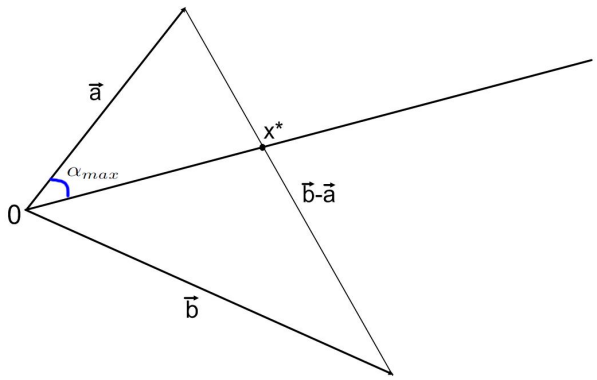

Figure 4.1: Maximal turning rate

combination of $\vec{a}$ and $\vec{b}$ that has the maximal turning angle with respect to $\vec{a}$, see Figure 4.1. In the constant speed case, $||\vec{a}|| = ||\vec{b}||$.

Proposition 2. *Let $\alpha_{max} \in (0, \pi)$ and let $\vec{a}, \vec{b} \in \mathbb{R}^n$ be linear independent vectors such that the angle between them is larger than α_{max}. Then the vector among the convex combination of $\vec{a}$ and $\vec{b}$ that has angle α_{max} with respect to $\vec{a}$ is given by*

$$\vec{x}^* = \lambda\vec{b} + (1-\lambda)\vec{a} \tag{4.2.1}$$

with $\lambda = \lambda_+$ or $\lambda = \lambda_-$ in $[0,1]$ given by

$$\lambda_\pm = \frac{||a||^2}{||a||^2 - \langle b, a\rangle \mp |\cot\alpha_{max}|\sqrt{||a||^2||b||^2 - \langle b, a\rangle^2}}. \tag{4.2.2}$$

Proof. It holds that

$$\begin{aligned} \vec{x}^* &= \vec{a} + \lambda(\vec{b} - \vec{a}) \\ &= \lambda\vec{b} + (1-\lambda)\vec{a} \end{aligned} \tag{4.2.3}$$

where $\lambda \in [0,1]$.
We know that the angle between $\vec{a}$ and $\vec{x}^*$ is the maximal angle, α_{max}, so this gives a second equation, with $c = \cos(\alpha_{max})$

$$\langle \vec{x}^*, \vec{a}\rangle = ||\vec{a}|| \cdot ||\vec{x}^*|| \cdot c. \tag{4.2.4}$$

Now by combining (4.2.3) and (4.2.4) and noting that

$$\langle \vec{x}^*, \vec{a}\rangle = \lambda\langle \vec{b}, \vec{a}\rangle + (1-\lambda)||\vec{a}||^2$$

we find that λ has to satisfy

$$\lambda\langle \vec{b}, \vec{a}\rangle + (1-\lambda)||\vec{a}||^2 = ||\vec{a}|| \cdot ||\vec{x}^*|| \cdot c. \tag{4.2.5}$$

By taking the square of equation (4.2.5) and using

$$\begin{aligned} ||x^*||^2 = \langle x^*, x^* \rangle &= (\lambda\vec{b} + (1-\lambda)\vec{a}) \cdot (\lambda\vec{b} + (1-\lambda)\vec{a}) \\ &= \lambda^2||\vec{b}||^2 + 2\lambda(1-\lambda)\langle\vec{b},\vec{a}\rangle + (1-\lambda)^2||\vec{a}||^2 \end{aligned}$$

we obtain after simplification:

$$\begin{aligned} \lambda^2\left[\langle b,a\rangle^2 - 2\langle b,a\rangle||a||^2(1-c^2) + ||a||^4(1-c^2) - c^2||a||^2||b||^2\right] & \\ +2\lambda\left[\langle b,a\rangle||a||^2(1-c^2) - ||a||^4(1-c^2)\right] - ||a||^4(1-c^2) &= 0 \\ \lambda^2\left[\left\{\langle b,a\rangle^2 - 2\langle b,a\rangle||a||^2 + ||a||^4\right\}(1-c^2) + c^2\left\{(b\cdot a)^2 - ||a||^2||b||^2\right\}\right] & \\ +2\lambda(1-c^2)\left[\langle b,a\rangle||a||^2 - ||a||^4\right] - ||a||^4(1-c^2) &= 0 \end{aligned}$$

Division by $(1-c^2)$ yields the quadratic equation in λ:

$$\begin{aligned} \lambda^2\left[\langle b,a\rangle^2 - 2\langle b,a\rangle||a||^2 + ||a||^4 + \frac{c^2}{1-c^2}\left\{\langle b,a\rangle^2 - ||a||^2||b||^2\right\}\right] & \\ +2\lambda\left[\langle b,a\rangle||a||^2 - ||a||^4\right] - ||a||^4 &= 0 \end{aligned} \tag{4.2.6}$$

Notice that the discriminant is given by

$$D = 4||a||^4\frac{c^2}{1-c^2}(||a||^2||b||^2 - \langle a,b\rangle^2) \tag{4.2.7}$$

where $\frac{c^2}{1-c^2} > 0$, since $c \in (-1,1)$. By using the Cauchy-Schwarz inequality $|\langle a,b\rangle| \leq ||a|| \cdot ||b||$ we conclude that $D \geq 0$.
Since $c = \cos\alpha_{max}$, we find

$$\frac{c^2}{1-c^2} = \frac{\cos^2\alpha_{max}}{1-\cos^2\alpha_{max}} = \frac{\cos^2\alpha_{max}}{\sin^2\alpha_{max}} = \cot^2\alpha_{max} \tag{4.2.8}$$

which brings us to

$$\begin{aligned} \lambda_\pm &= \frac{||a||^4 - \langle b,a\rangle||a||^2 \pm ||a||^2|\cot(\alpha_{max})|\sqrt{||a||^2||b||^2 - \langle a,b\rangle^2}}{(||a||^2 - \langle b,a\rangle)^2 - \cot(\alpha_{max})^2(||a||^2||b||^2 - \langle b,a\rangle^2)} \\ &= \frac{||a||^2}{||a||^2 - \langle b,a\rangle \mp |\cot(\alpha_{max})|\sqrt{||a||^2||b||^2 - \langle b,a\rangle^2}}. \end{aligned} \tag{4.2.9}$$

□

Application in $\mathbb{R}^3$
The result of Proposition 2 is useful for us in $\mathbb{R}^3$ since we can simplify λ even further by using the cross product. By using φ as the angle between $\vec{a}$ and $\vec{b}$ and the common relations

$$\begin{aligned} \langle b,a\rangle &= \cos\varphi \cdot ||a|| \cdot ||b|| \\ |a\times b| &= |\sin\varphi| \cdot ||a|| \cdot ||b|| \\ |a\times b|^2 &= ||a||^2||b||^2 - \langle a,b\rangle^2, \end{aligned}$$

we can simplify (4.2.9) in order to get

$$\begin{aligned} \lambda_{\pm} &= \frac{||a||}{||a|| - ||b||(\cos\varphi \pm |\cot\alpha_{max}||\sin\varphi|)} \\ &= \frac{||a||}{||a|| - ||b|| \cdot |\sin\varphi|(\cot\varphi \pm |\cot\alpha_{max}|)}. \end{aligned} \tag{4.2.10}$$

Since $0 < \alpha_{max} < \varphi \leq \pi$, $\sin\varphi \geq 0$. Notice that

$$[\cot x]' = \left[\frac{1}{\tan x}\right]' = -\frac{1}{\tan^2 x}\frac{1}{\cos^2 x} < 0, \tag{4.2.11}$$

so $\cot x$ is a decreasing function. Hence $\cot\varphi < \cot\alpha_{max}$ and $\cot\varphi - \cot\alpha_{max} < 0$. Now we notice that $\lambda_- > 0$. In the constant speed case, $||a|| = ||b||$ and λ_- can be written as $\frac{||a||}{k||a||} = \frac{1}{k}$ with $k > 1$. Hence $\lambda_- < 1$. On the other hand, if $\lambda_+ > 0$, we can also write it as $\frac{||a||}{k||a||} = \frac{1}{k}$, but now $k < 1$, so $\lambda_+ \notin [0, 1]$. Concluding, our unique suitable $\lambda \in [0, 1]$ is given by:

$$\lambda = \frac{||a||}{||a|| - ||b|| \cdot \sin\varphi(\cot\varphi - \cot\alpha_{max})}. \tag{4.2.12}$$

Finally, notice that if $\varphi = \pi$, $\cot\varphi$ is not defined. In that case, we can conclude from (4.2.10) that $\lambda = \frac{1}{2}$ which means that the fish prefers to stay where it is. In this case, the fish will make a maximal turn in a random direction to avoid collision.
Now we have found our x^* and by scaling it to the (constant) speed, we find our new position.

4.3 Water surface and sea floor

Most models that are mentioned in the modelling overview in [17] use a bounded area or square lattice. However, it is not mentioned which and how boundary conditions are incorporated.
In order to make model predictions accessible to experimental validations, we have included a water surface and a sea floor in our simulation as vertical boundary conditions. Just underneath the water surface we have added a layer, in which fish will start to adjust their direction to prevent jumping out of the water. A similar layer above the sea floor is included to prevent collision.
The maximal turning angle of the fish (Section 4.2) imposes a condition on the thickness b of this layer. It must have a thickness that is at least so, that fish can correct their movement direction with several turns of maximal angle and stay in the water, or not hit the bottom of the tank or sea floor. In order to determine the minimal value of b, b_{min}, we first look at the worst-case scenario for a single fish: it is entering this layer swimming straight upwards. In this case, the fish wants to make several maximal turns downwards with angle α_{max}. After the first step, the difference in vertical position, Δz_1, is equal to $s_i\Delta\tau\cos\alpha_{max} = s_i\Delta\tau\sin(\frac{1}{2}\pi - \alpha_{max})$. The reason we use this last notation is to be consistent with the spherical coordinates used on the sphere of perception:

φ is the elevation angle measured from the xy-plane. Similar, the second step gives an additional vertical shifting of $\Delta z_2 = s_i \Delta\tau \sin(\frac{1}{2}\pi - 2\alpha_{max})$, see Figure 4.2A. Proceeding this iteratively and stopping when $\frac{1}{2}\pi - n\alpha_{max} < 0$, we need

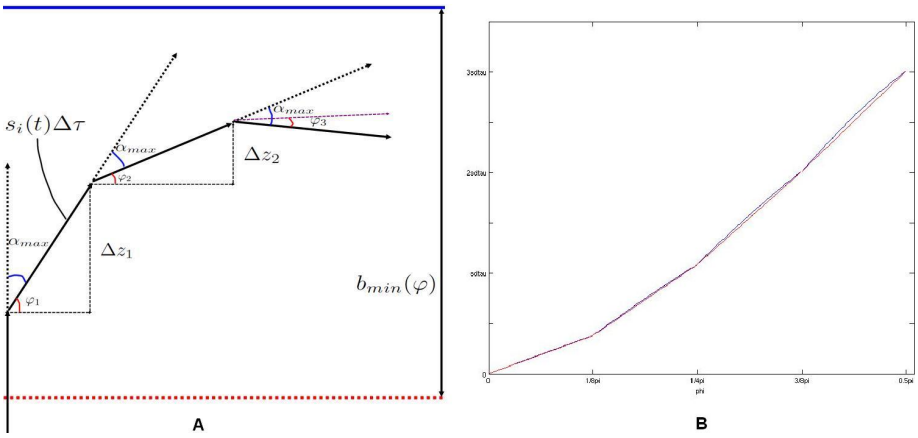

Figure 4.2: A: Layer underneath the water surface. B: Graph of function $b_{min}(\varphi)$ for $\alpha_{max} = \frac{1}{8}\pi$ and a piecewise linear approximation (in red).

to start turning at a level b_{min} underneath the water surface where in the worst case scenario of $\varphi = \frac{1}{2}\pi$ it holds that

$$b_{min} = \sum_{n\in\mathbb{N}_0} \Delta z_n = s\Delta\tau \cdot \left(\sum_{n\in\mathbb{N}_0 : \frac{1}{2}\pi - n\alpha_{max} \geq 0} \sin(\frac{1}{2}\pi - n\alpha_{max}) \right) \tag{4.3.1}$$

where $s = \max s_i$. Note that per fish the speed s_i is constant. It may be equal for all fish.

We can use this method to determine the minimal thickness of the boundary layer for fish entering this layer under an angle $\varphi \in [0, \frac{1}{2}\pi]$ with the xy-plane. For $\varphi \in [-\frac{1}{2}\pi, 0]$ it is not necessary to change its direction to prevent jumping out of the water since it is already swimming downwards.
Hence we find for $\varphi \in [0, \frac{1}{2}\pi]$:

$$\begin{aligned} b_{min}(\varphi) = \sum_{n\in\mathbb{N}_0} \Delta z_n &= s\Delta\tau \cdot \left(\sum_{n\in\mathbb{N}_0 : \varphi - n\alpha_{max} \geq 0} \sin(\varphi - n\alpha_{max}) \right) \\ &= s\Delta\tau \cdot B_{min}(\varphi). \end{aligned} \tag{4.3.2}$$

In Figure 4.2B this function is drawn for $\alpha_{max} = \frac{1}{8}\pi$. Note that this function can be approximated well by a piecewise linear function.

Lemma 1. *The function $\varphi \mapsto b_{min}(\varphi)$ is strictly increasing and continuous on $[0, \frac{1}{2}\pi]$. In particular it is injective.*

Proof. First note that we can rewrite equation (4.3.2) using

$$\begin{aligned} B_{min}(\varphi) &= \sum_{n=0}^{\infty} \mathbf{1}_{[n\alpha_{max}, \frac{1}{2}\pi]}(\varphi) \cdot \sin(\varphi - n\alpha_{max}) \\ &= \sum_{n=0}^{\infty} f_n(\varphi). \end{aligned}$$

It holds that each function $\varphi \mapsto f_n(\varphi)$ is continuous on $[0, \frac{1}{2}\pi]$. The sum is finite, so $B_{min}(\varphi)$ is continuous and hence $b_{min}(\varphi)$ is continuous.

Let $0 \leq \varphi_1 < \varphi_2 \leq \frac{1}{2}\pi$ and let $n_i := \max\{n \in \mathbb{N}_0 : n\alpha_{max} \leq \varphi_i\}$. Then $n_2 \geq n_1$. Now it holds that

$$\begin{aligned} B_{min}(\varphi_2) - B_{min}(\varphi_1) &= \sum_{k=0}^{n_2} \sin(\varphi_2 - k\alpha_{max}) \\ &\quad - \sum_{k'=0}^{n_1} \sin(\varphi_1 - k'\alpha_{max}) \\ &= \sum_{k=0}^{n_1} [\sin(\varphi_2 - k\alpha_{max}) - \sin(\varphi_1 - k\alpha_{max})] \\ &\quad + \sum_{k'=n_1+1}^{n_2} \sin(\varphi_2 - k'\alpha_{max}). \end{aligned} \tag{4.3.3}$$

Since $\varphi_i - k\alpha_{max} \in [0, \frac{1}{2}\pi]$ for $k = 0, 1, \cdots, n_1$ and $\varphi \mapsto \sin\varphi$ is strictly increasing on $[0, \frac{1}{2}\pi]$, the first sum over k in (4.3.3) is strictly positive. The second sum is non-negative. Therefore $b_{min}(\varphi_2) > b_{min}(\varphi_1)$.
Hence $b_{min}(\varphi)$ is a strictly increasing continuous function. □

Let z_w be the z-coordinate of the water surface. At every time step, we check for every fish whether its swimming depth $z_w - z_i(t)$ and the vertical angle $\varphi(t)$ are such that $z_w - z_i(t) > b_{min}(\varphi(t))$. If not, we will need to adjust its vertical angle such that $z_w - z_i(t) > b_{min}(\varphi(t))$. That is, from the next step onwards, it is able to stay under water.
We assume that this condition was fulfilled in the previous time step, so we know that it is possible for the fish to stay under water by making several maximal turns. At every vertical position, we know what the maximal vertical angle φ_{max} can be, using equation (4.3.2) and Lemma 1, see Figure 4.2B, by inverting b_{min}. In the implemented simulation we use a piecewise linear approximation for b_{min}, which is reasonably in view of Figure 4.2B.
That is why we check if the vertical angle of desired direction of the fish, φ, is smaller than φ_{max}. If this is not the case, the virtual fish needs to adjust its direction more downwards and adopt this maximal vertical angle. This can be done by using the same construction used for the maximal turning angle α_{max}. Then we take the desired direction vector as $\vec{a}$, its horizontal projection as $\vec{b}$ and our $\vec{x}^*$ is now placed on the vector which has angle φ_{max} with $\vec{b}$ and smallest angle with $\vec{a}$. According to Proposition 2 there is a unique position which satisfies the conditions.

At this point we need to be careful: if a fish needs to make a maximal turn in vertical direction, this means that the horizontal angle must be zero. Hence, it is not correct to only adjust the vertical angle, we also need to take the horizontal angle into account, since the combination of these leads to the angle α between the direction of fish i at time t, $d_i(t)$, and its direction at time $t+1$, $d_i(t+1)$ which cannot exceed α_{max}.
At every vertical position z, we know the maximal vertical angle, φ_{max}, a fish can have when swimming at this level with speed s, since b_{min} is invertible as a strictly increasing continuous function. In fact;

$$\begin{aligned} \varphi_{max} &= \varphi_{max}(z,s) = b_{min}^{-1}(z_w - z) \\ &= B_{min}^{-1}(\frac{z_w - z}{s\Delta\tau}). \end{aligned}$$

We need to check two things:

1) Does $\varphi_i'(t+1)$, the angle between the desired direction $d_i'(t+1)$ and the xy-plane, satisfy

$$B_{min}(\varphi_i'(t+1)) > \frac{z_w - z_i(t)}{s\Delta\tau}; \tag{4.3.4}$$

(4.3.5)

2) Does the angle between $d_i(t)$ and $\tilde{d}_i(t+1)$, the direction vector after adjusting φ' to $\tilde{\varphi}$ to satisfy 1), not exceed the maximal turning angle, i.e. does it hold that $\cos(\alpha) = \tilde{d}_i(t+1) \cdot d_i(t) \leq \cos(\alpha_{max})$?

If condition 1) is not satisfied, we have to adjust φ' to φ_{max}. If by adjusting φ', α exceeds α_{max}, we also need to adjust ϑ to secure that $\alpha \leq \alpha_{max}$.
Let $a = d_i(t), b = d_i'(t+1)$ and $b' = \tilde{d}_i(t+1)$ the new direction vector with maximal vertical angle. Assume that $||a|| = ||b|| = ||b'|| = 1$ and note that

$$a = \begin{bmatrix} x_a \\ y_a \\ z_a \end{bmatrix} = \begin{bmatrix} \cos(\varphi_a)\cos(\vartheta_a) \\ \cos(\varphi_a)\sin(\vartheta_a) \\ \sin(\varphi_a) \end{bmatrix}.$$

Then we want to solve for the vector b'

$$\begin{aligned} \cos(\alpha_{max}) &= a \cdot b' \\ &= \cos(\varphi_a)\cos(\vartheta_a)\cos(\varphi_{b'})\cos(\vartheta_{b'}) \\ &\quad + \cos(\varphi_a)\sin(\vartheta_a)\cos(\varphi_{b'})\sin(\vartheta_{b'}) \\ &\quad + \sin(\varphi_a)\sin(\varphi_{b'}), \end{aligned} \tag{4.3.6}$$

where all the parameters are known except $\vartheta_{b'}$. Note that $\varphi_{b'} = \varphi_{max}(z,s)$. We can rewrite equation (4.3.6)

$$c_1 = c_2\cos(\vartheta_{b'}) + c_3\sin(\vartheta_{b'}) \tag{4.3.7}$$

where

$$\begin{aligned} c_1 &= \cos(\alpha_{max}) - \sin(\varphi_a)\sin(\varphi_{max}), \\ c_2 &= \cos(\varphi_a)\cos(\vartheta_a)\cos(\varphi_{max}), \\ c_3 &= \cos(\varphi_a)\sin(\vartheta_a)\cos(\varphi_{max}). \end{aligned}$$

It holds that

$$c_2 \cos(\vartheta_{b'}) + c_3 \sin(\vartheta_{b'}) \quad = \quad \sqrt{c_2^2 + c_3^2} \cdot \sin(\vartheta_{b'} + \beta) \tag{4.3.8}$$

with

$$\beta = \arctan\left(\frac{c_2}{c_3}\right) + \begin{cases} 0 & \text{if} \quad c_3 \geq 0, \\ \pi & \text{if} \quad c_3 < 0. \end{cases}$$

Hence we can calculate the horizontal angle $\vartheta_{b'}$ for b' by

$$\begin{aligned} \vartheta_{b'} &= \arcsin\left(\frac{c_1}{\sqrt{c_2^2 + c_3^2}}\right) - \beta \qquad \text{or} \\ \vartheta_{b'} &= \pi - \left(\arcsin\left(\frac{c_1}{\sqrt{c_2^2 + c_3^2}}\right) - \beta\right) \end{aligned} \tag{4.3.9}$$

where we choose $\vartheta_{b'}$ for equation (4.3.9) such that the deviation from $d_i'(t+1)$ is minimal. The resulting vector b' has $\varphi' = \varphi_{max}$ and turning angle $\alpha \leq \alpha_{max}$. We have made a similar construction to avoid collision with the sea floor.

Chapter 5

A variable speed model

In the previous sections we have used a constant speed in our model. Now we are ready to make our model more realistic, by making the speed of the fish variable. This is not as simple as it may seem, in particular because we want to have experimentally verifiable expressions. How is this speed related to the state the fish is in, its body length and other aspects? The vertical boundary conditions also depend on the speed, so how do these change when the speed is made variable? A large fish will swim faster than a small fish since the distance traveled by one tail beat is given by $0.7BL$, [5], so the speed must be related to the length of the fish in our model.
In our model, we let every fish start with its favorite cruising speed. In the literature there are different approaches for this speed. According to [5], $s_{fav} = 0.5BL^{0.43}$ where BL is in m and s_{fav} in cm/s, which corresponds with the expectations based on minimal energy expenditure, whereas in [3] they use $s_{fav} = g^{1/2}\rho_b^{-1/6}M_b^{1/6}$ where g, ρ_b, M_b represent respectively the acceleration of gravity, body density and body mass. In [21], Videler relates the optimal cruising speed to the mass of the fish by $s_{fav} = 0.47M^{0.17}$ with M in kg and s_{opt} in cm/s. Obviously, these approaches for the favorite cruising speed were constructed to fit particular experimental data.
In this section we will discuss how the speed changes through time, depending on the state the fish is in. How much power it wants to invest in acceleration will be investigated first, followed by the rules on how to adjust the velocity. In Chapter 6 we will compare the simulation results of this variable speed model and the constant speed model.

5.1 Decision making: the desired direction

Once we have stored the observed environment on the sphere of perception, we need to use it to determine where the fish wants to go in the next time step. Since we use spherical coordinates, we can rewrite our desired direction

as described in Section 4.1 as

$$\begin{aligned} d' &= \int_{S^2} \omega f(\omega) \mathrm{d}\omega \\ &= \int_{\varphi=-\frac{1}{2}\pi}^{\frac{1}{2}\pi} \int_{\vartheta=-\pi}^{\pi} \Phi(\vartheta,\varphi) f(\vartheta,\varphi) |\partial\Phi(\vartheta,\varphi)| d\vartheta d\varphi \end{aligned} \tag{5.1.1}$$

where

$$\Phi(\vartheta,\varphi) = \begin{bmatrix} r\cos\varphi\cos\vartheta \\ r\cos\varphi\sin\vartheta \\ r\sin\varphi \end{bmatrix} = \begin{bmatrix} \cos\varphi\cos\vartheta \\ \cos\varphi\sin\vartheta \\ \sin\varphi \end{bmatrix}$$

since $r = 1$ and

$$\begin{aligned} |\partial\Phi(\vartheta,\varphi)| &= \left| \frac{\partial\Phi}{\partial\vartheta} \times \frac{\partial\Phi}{\partial\varphi} \right| \\ &= \sqrt{\cos^4(\varphi) + \cos^2(\varphi)\sin^2(\varphi)[\cos^4(\vartheta) + \sin^4(\vartheta)] + 2\cos^2(\varphi)\sin^2(\varphi)\cos^2(\vartheta)\sin^2(\vartheta)} \\ &= \sqrt{\cos^4(\varphi) + \cos^2(\varphi)\sin^2(\varphi)[\cos^2(\vartheta) + \sin^2(\vartheta)]^2} \\ &= \sqrt{\cos^2(\varphi)} = |\cos(\varphi)|. \end{aligned}$$

Notice that $|\partial\Phi(\vartheta_k,\varphi_l)|\Delta\vartheta\Delta\varphi \approx A_{k,l}$, the surface area of the part of the sphere corresponding to the 'box' in spherical coordinates designated by ϑ_k, φ_l. By approximating the integral by a Riemann sum, equation (5.1.1) becomes

$$\begin{aligned} d' &\approx \sum_{k,l} \Phi(\vartheta_k,\varphi_l) f(\vartheta_k,\varphi_l) |\partial\Phi(\vartheta_k,\varphi_l)| \Delta\vartheta\Delta\varphi \\ &= \sum_{k,l} \Phi(\vartheta_k,\varphi_l) f(\vartheta_k,\varphi_l) |\cos(\varphi_l)| \Delta\vartheta\Delta\varphi \\ &= \sum_{k,l} \Phi(\vartheta_k,\varphi_l) f(\vartheta_k,\varphi_l) A_{k,l} \end{aligned}$$

and

$$\hat{d'} = \frac{d'}{||d'||}.$$

In Section 4.1 we have shown that this is comparable with the model used by Couzin and others when fish do not 'overlap', but what happens if the do neighbours overlap, are hidden behind each other, and will hence give an overlapping spot on the sphere of perception? Then it is no longer correct to just add all the different direction vectors and equation (5.1.1) will give a different outcome than the model by Couzin.
This is one point where our model differs from previous models. This approach will give a more realistic outcome, compared to previous models.

5.2 Adjusting speed and direction

How fish modify their direction and speed depends highly upon the particular species considered, as different species may use different swimming and steering

techniques [5,21]. Consequently, when modelling a particular species in an experimental setting, this part needs to be 'filled in' based upon observations and measurements of these techniques. Since we lack such relation to experiment here unfortunately, we shall illustrate the way one may proceed at this point using a hypothetical example.
As in Section 3.3 we consider a pelagic fish like tuna that can be considered as a rigid body with an oscillating propeller. The latter is able to generate a forward thrust power P^{thrust}. One issue, which should be settled through experimental observations, is to what extent the fish is able to both generate forward thrust and steer at the same time. In the extreme case, a fish must alternate between a period of (forward) acceleration and a period of steering, in which the tail fin is held at a particular angle θ and the fish is loosing kinetic energy at a rate $P^{steering}(v_t, \dot{\theta})$, as described in Section 3.2. Possibly steering and forward thrust may be combined, be it that P^{thrust} is lower in this case, depending on the angular velocity ω of the steering movement. In any case it is important to know the thrust power that the fish is able or 'willing' to generate in that situation. The power loss due to steering can be resolved from biophysical considerations along the lines of reasoning of Section 3.3.
Thus, when P^{thrust} is known, the new speed and direction after one time step can be computed.

5.3 Thrust power distribution

We postulate below how much thrust power a fish would invest in locomotion, depending on the mood it is in. If a fish is in a life threatening situation, it will do everything it can to prevent being caught by a predator and hence invest its maximal power, if necessary. If a fish is foraging, the displacement is small and hence it will not use a lot of power. When cruising from one place to another, it would like to keep its favorite cruising speed and direction. This way the change in kinetic energy remains zero, and from equation (3.2.3) it follows that it wants to keep its power close to $\frac{1}{2}C|v(t)|^3$. While being attracted by a school, it will also invest power in catching up with this school. Finally, if it is trying to avoid its neighbours, it will still prefer to keep its cruising speed while minimizing the required power, but now with a larger standard deviation; if necessary it will avoid collision at the expense of saving energy. In Figure 5.1 we have translated our assumptions into examples of distributions for different moods of the fish.
We are interested in the functions to describe these distributions. Notice that the power invested will never be negative, so we need positive functions. A possibility is the log normal distribution: this is a probability distribution of a random variable whose logarithm is normally distributed. Ergo, if $Y \sim N(\mu, \sigma^2)$, then $X = e^Y \sim \log N(\mu, \sigma^2)$. When for example $\sigma \sim 10$, this describes the foraging mood; fish swim in all directions. When cruising around, fish swim in mainly the same direction and at the same speed and hence invest around the same amount of power, which explains the second distribution. The remaining moods are similar to the latter, but have different mean, since fish will invest more power in life threatening situations and to catch up with a school than it would while just cruising around. Notice that this power is bounded from above by the maximal power possible to invest.

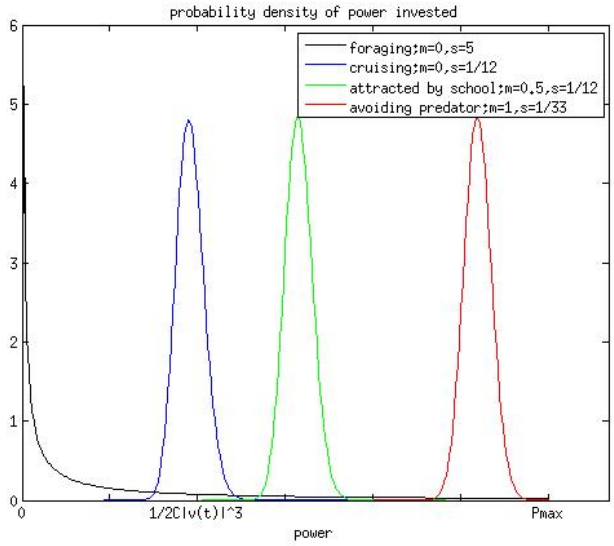

Figure 5.1: Example of a power distribution in different behavioural situations ('moods').

When the fish and environment depend parameter C is known, these distributions can be used to determine how a fish will change its speed, as explained in Section 3.2.

5.4 Speed adjustment in implementation

Since we do not model and simulate one specific fish type and lack experimental observations and data on this point, we will adjust the speed in a more straight forward way. We use different rules to adjust the speed in the various aggregation zones. Let us first look at the speed adjustment in the smallest zone, the zone of repulsion. According to Hemelrijk [9], fish will slow down in this zone. They already change direction to prevent collision, but in order to deviate as little as possible from the desired direction, they will slow down. The new speed can be constructed using

$$s_i(t+1) \quad = \quad \frac{1}{3}\left(s_{fav} + s_i(t) + s_{min}\right), \tag{5.4.1}$$

where s_{min} depends on the acceleration of the fish; it is the minimal speed possible to attain in one time step when slowing down maximally.
If there are only fish in the zone of alignment, it will adjust its speed to the n neighbours in this zone, while also trying to return to its favorite cruising speed:

$$s_i(t+1) = \frac{1}{3}\left(s_{fav} + s_i(t) + \frac{1}{n}\sum_{j=1}^{n} s_j(t)\right). \tag{5.4.2}$$

Note that directional information has been incorporated in the desired direction already.
While aligning with its neighbours in the alignment zone, fish still want to get close to larger groups in the neighbourhood. If there are also neighbours in the zone of attraction, fish want to adjust their speed as mentioned in equation (5.4.2), but also accelerate to catch up with the school. In that case we can adjust equation (5.4.2) in order to get

$$s_i(t+1) = \frac{1}{3}\left(s_{fav} + s_i(t) + \frac{n}{n+m}\frac{1}{n}\sum_{j=1}^{n} s_j(t) + \frac{m}{m+n}s_{max} \right)$$

where s_{max} represents the desired speed to catch up with the school. We weigh the last two terms; if the fraction of neighbours in the alignment zone is very small compared to the number of neighbours in the attraction zone, the fish will be more inclined to speed up, whereas if it is the other way around, it will prefer to adjust its speed to the neighbours in the alignment zone.
As we have seen in Section 5.3, if there are only fish in the largest interaction zone, the zone of attraction, the invested power will be larger than $\frac{1}{2}C|v(t)|^3$ and hence it will accelerate. How much it will accelerate might depend on the size of the school it is approaching and the perceived distance to the school. For simplicity, both s_{min} and s_{max} have been taken constant in our model.
If there are no fish to interact with, the total power encountered by the fish will stay close to zero. Hence the change in velocity is negligible in this case and we will add a little noise to the speed at time t to find the speed at time $t+1$. We will apply the magnitude of the new velocity in the desired direction. Hence it will adjust its speed as in equation (5.4.1).

5.5 Implementation of boundary conditions

The realisation of the water surface and sea floor boundary in the constant speed model used a 'boundary layer' of a thickness that depended on the speed of fish, see Section 4.3. The best way to adjust the speed when a fish is entering this layer, is to slow down. This way, it is not forced to make a lot of large turns in a row, and deviate as little as possible from its desired direction. We used this approach in our implementation.

Chapter 6

Simulation results

To investigate our simulation results, we plotted the movement of our artificial fish in four frames: one three dimensional plot and three projections on the xy-, yz- and xz-plane respectively, see Figure 6.1. To make the distinction in body length of the fish, we have added colors: blue represents small fish, green fish with body length close to average, and red large fish.
This enables us to get a good impression of how our artificial fish swim, see Figure 6.1 and Figure 6.2 for an example. There we have plotted four subsequent moments of the variable speed model comparable to Couzin's model, but then with vertical boundary conditions and the perceived distance instead of the absolute distance to the neighbours.

6.1 Time series for 3D plots

In Figure 6.1 and 6.2 we plot a simulation run at four subsequent time points, starting from a random configuration at $t = 1$. Initial positions have been chosen homogeneously, similarly for directions. Every fish starts with it favorite cruising speed, depended on the body length, which is normally distributed. The small and large fish deviate more than one standard deviation from the mean body length. More parameter settings are listed in Table 6.1.

From these plots it is hard to compare the simulation results of our models. Therefore we investigate how the horizontal and vertical direction of the fish changes through time. In the variable speed model, we also investigate how the speed changes through time. We were interested in the influence of the vertical boundaries on the results of the simulation and if and how our model based on the sphere of perception differs from the model with the perceived distance.

6.2 Horizontal and vertical direction distributions

In both the constant speed model and the variable speed model we make the distinction between the model with periodic boundary conditions in all directions, and the model which includes the water surface and the sea floor. We investigated the orientation of every fish at every time step in both horizontal and vertical direction.

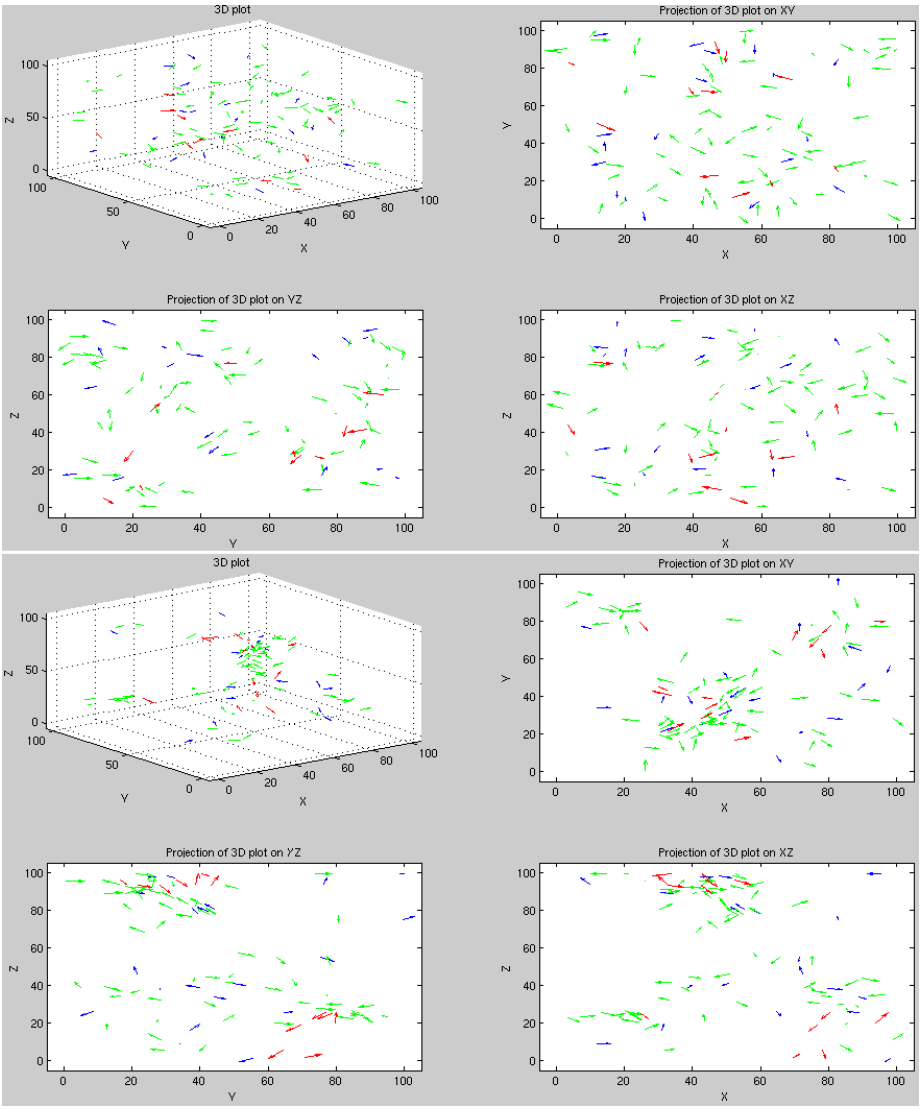

Figure 6.1: Example of the state at two subsequent time points in our simulation with vertical impenetrable boundary conditions and horizontal periodic boundaries (t=1 and t=100 approximately).

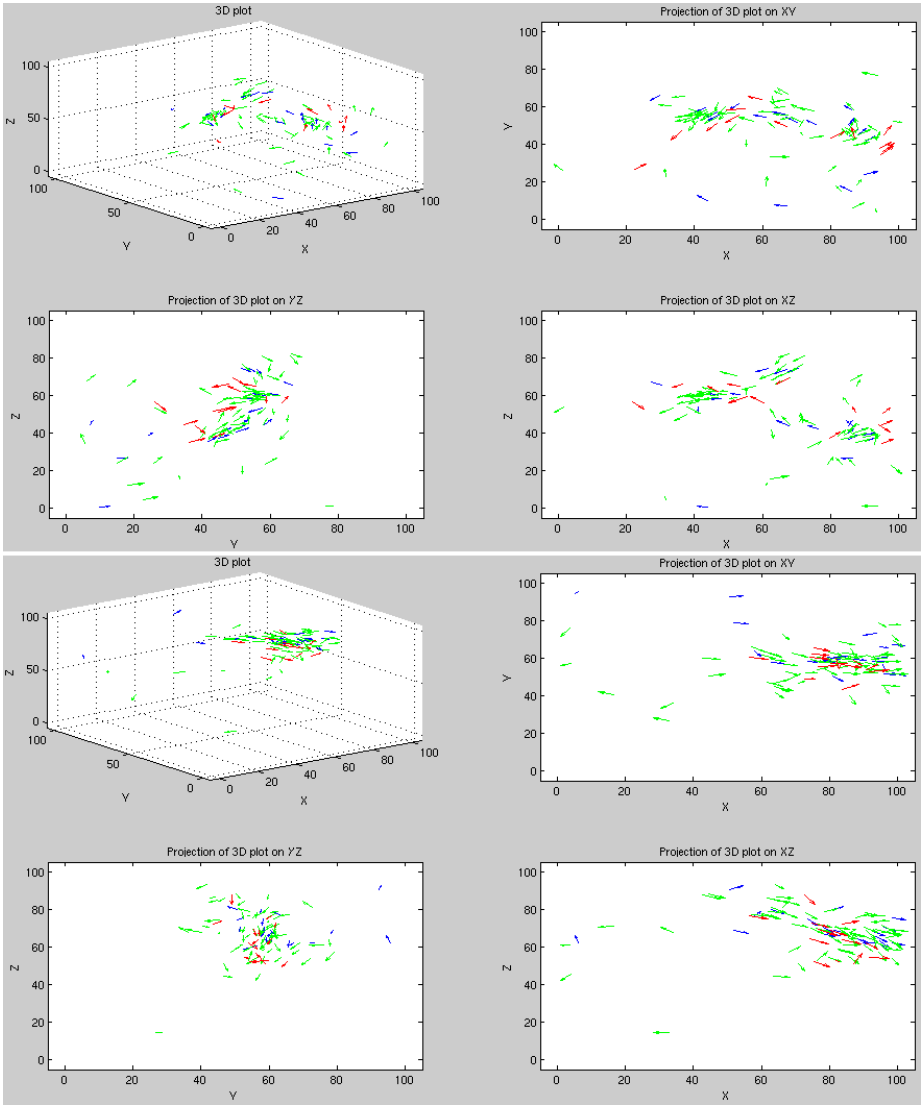

Figure 6.2: Two more time steps at time t=200 and t=400 approximately.

The main difference in schooling behaviour in the model with periodic boundary conditions was that it took more time to school compared to the model with vertical boundaries. Since fish at the top of the (virtual) tank are only attracted by fish below them, and fish at the bottom only by fish above them, this resulted in a contraction of all fish towards the centre of the tank, which is visible in the example plotted in Figure 6.1 and Figure 6.2. In the model with periodic boundary conditions, fish at the top were also attracted by fish 'above' them, which were placed at the bottom of the tank. This caused more chaos to start with, but eventually it resulted in the same behaviour as the more realistic model with incorporated water surface and sea floor. This result was visible in both the constant speed and the variable speed model. Since speed was variable

Table of parameters

Parameter	Unit	Symbol	Value
Number of fish	1	N	50-100
Time step	s	$\Delta\tau$	$\frac{1}{30}$
Length of fish	cm	BL	5
Velocity	BL/s	v	0-s_{max}
Favorite cruising speed	BL/s	s_{fav}	3
Maximum speed	BL/s	s_{max}	5
Minimum speed	BL/s	s_{min}	0.5
Radius of zone of repulsion	BL	ρ	0.5
Radius of zone of alignment	BL	α_1	2
Radius of zone of attraction	BL	α_2	5
Maximal turning angle	rad	α_{max}	$\frac{1}{8}\pi$
Depth and width of water tank	BL	size	20
Size of box of grid representing sphere of perception	1	M	20

Table 6.1: Table of parameters

in the latter, this led to faster aggregation behaviour. In Figure 6.3 we have plotted histogram of the horizontal and vertical orientation of 100 fish for 200 time steps in the constant speed model with vertical boundaries. Since every run starts with random position and orientation for all fish, the output of other runs may vary. Note that the vertical orientation is mainly zero. This is caused by the periodic boundaries, since vertical movement is restricted in certain areas of the virtual tank. The vertical orientation in the models without vertical boundaries was more scattered. We have used the typical values according to Huth and Wissel [12] of the three zones: repulsion zone $0.5BL$, alignment zone $2BL$ and the attraction zone $5BL$. Recall from Section 3.1 that these zones can be made more precise if the type of fish investigated is specified. When we make the repulsion zone smaller, this results in a more aligned school and hence in a higher and steeper peak in the orientation plots. A larger attraction zone might lead to chaos, since fish get attracted to too many sides to determine a new direction. A too small attraction zone will slow down the aggregation process. The same holds for the alignment zone.

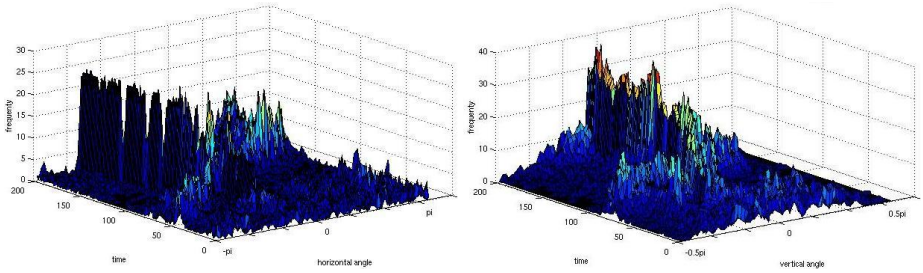

Figure 6.3: Histogram of horizontal and vertical orientation of 100 fish through time resulting from the constant speed model with horizontal periodic boundaries and water surface and sea floor restrictions.

The model including the sphere of perception yielded a slightly different output,

since it took more time for fish to school. This can be explained by the part that neighbours hidden behind others are not visible. Hence, if a neighbouring fish is really close, the amount of fish influencing the decision of a fish is a lot smaller which will slow down the aggregation process.
Movies of simulation output for the various models are available in the supplementary material, see Appendix B.

6.3 Speed distribution

Beside the orientation, we are also interested in how the speed changes through time and how this depends on the boundary conditions. In our simulation, every fish starts with its favorite cruising speed. When starting the simulation, we see that all the fish start to accelerate immediately in order to get closer to other fish. After a while, fish do not need to accelerate a lot any more, since they have become part of a school. At that point they start to return to their favorite cruising speed. Since they are still trying to keep the same speed as their neighbours and are constantly attracted by neighbours in the school, the entire school will eventually swim with a speed between the average cruising speed and the maximal speed caused by attraction, see Figure 6.4.

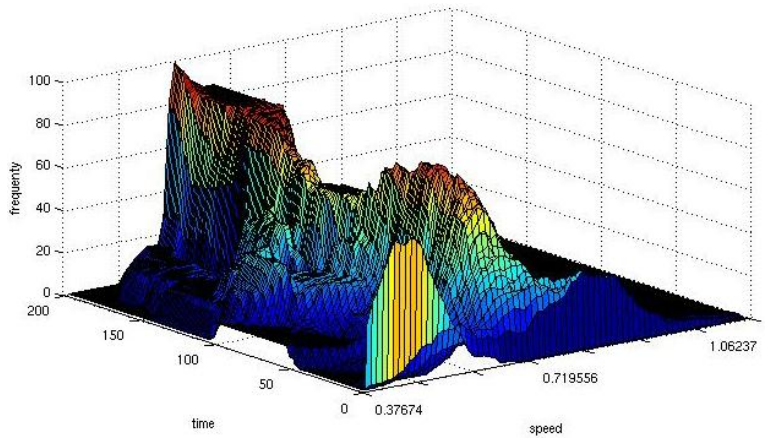

Figure 6.4: Change in speed distribution of the population over time.

Chapter 7

Discussion and proposals for further research

7.1 Discussion and conclusion

In this thesis we investigated multiple mathematical models made to model collective behaviour of living organisms. We can conclude that most models encountered in the literature originated from biology, but were further developed as 'toy-models', which had a poor relation to biology and lacking the possibility of validation by experimental data. We have tried to keep biology in focus when making our model, by building in different aspects in which experimental data can be incorporated. By carefully separating observation, decision making and physical response, we were able to get more insight in the aggregation process. In Section 3.1 we found a method to determine the sizes of the different regions around a fish better by using the visual observation system. We succeeded in implementing the boundary conditions at the water surface and the sea floor while taking the maximal turning angle into account. These are examples of aspects where we have made our model more realistic. Besides these improvements, we have used a completely different way of describing and storing the observed environment, by using the sphere of perception.

The result is a model with an outcome not completely different from other models, but completely different behind the scenes, in its 'architecture', and the way in which underlying processes like observation, decision making and response are explicitly modelled. From our simulations, we can conclude that we have proven our concept. The implementation of the sphere of perception and various aspects which can be adjusted to the type of fish, or other organism, investigated, still results in artificial fish acting similar to fish in nature. Hence our model is an improvement of existing models with a better relation to biology.

7.2 Proposal for further research

Further details on the biophysics of the fish visual system and possibly similarly for the lateral line, may result in a better explanation of the radii of the different aggregation zones, in view of (3.1.4). Note that in our approach to modelling the visual system, we neglect the dependence on depth of the effective radiant power in the (sun)light reflected on fish. This represents a well-lighted experimental set up in a fish tank. In a natural environment, lightning conditions will depend on the swimming depth, i.e. the deeper the fish swims, the more light will already be adsorbed by the water before being reflected on the fish. Moreover, the time of the day and the time of the year determine the position of the sun and therefore the amount of sunlight and the angle it is penetrating the water with. These aspects influence the amount of light reflected on fish and can be incorporated by replacing the average radiant power $\bar{p}$ from Section 3.1 by

$$\bar{p}' = \bar{p}_0 e^{-\alpha(z_w - z_t)} \tag{7.2.1}$$

where z_w and z_t are the z-coordinate of the water surface and the fish at time t respectively and $\bar{p}_0$ is the effective radiant power at the water level, which depends on the moment of the day and the time of the year.
It would be interesting to see whether this creates a preferred swimming depth for the fish and how this depends on the time of the day and year, the skin structure, body shape and eye sight properties. By making the distinction in body length visible in the simulation output, one might be able to draw conclusions about the influence of the body length on aggregation and show that artificial fish act the same way as in nature; fish which differ more than 30% is body size do not fit in the school.

Concluding, the approach described in Section 2.2 assumes deterministic decision moments at $t = \Delta t$. But we actually have no information about how often fish observe their environment and decide to adjust their velocity. Therefore it might be more realistic to take a distribution of the decision moments, for example a Poisson distribution. Another option is to take continuous decision moments which is the limit of de discrete decision moment case, but this is even more complicated.

We hope this model and modelling approach will be used in the future in order to explain typical aggregation behaviour in fish, or other organisms.

Appendix A

Pseudocode

```
function[]=fishschool(r1,a1,a2)
%fishschool simulation
%r1: (radius zone of repulsion)
%a1: (radius zone of alignment)
%a2: (radius zone of attraction)

%initial values
N;        %number of fish
T;        %time
size;     %size square(or kubed) grid
mu;       %average body length of fish
sigma;    %standard deviation
dtau;     %physical timestep
alphamax; %maximum turning angle per timestep
gamma;    %visionrange


%iv for differentiating fishsizes
small=mu-sigma;     %upper limit for small fish
big=mu+sigma;       %lower limit for big fish

%make first position
for i=1:N
*give fish i random position, (unit) direction and length
  *make size of zones depending on fish
  %in the variable speed model:
  *let fish start with its favorite cruising speed
  *determine maximal and minimal speed
end
*determine average body length

for t=1:T       %for all time steps
    for i=1:N   %for alle fish
        % determine for i its perceived environment
```

```
        *determine which fish are visible and with which intensity
        *and store this in the sphere of perception matrix

        % fish i makes decission what to do
        if there are neighbours in the zone of repulsion
         *integrate over the boxes filled by these fish and turn away
        else if there are neighbours in zone of alignment
         *adopt direction of fish in this zone
        if there are neighbours in zone of attraction
         *integrate over these boxes and change direction
        if there are no neighbours around, add some noise to the direction

        %check if new direction does not exceed alpha_max
        if it does, change direction such that angle is alpha_max

        %make new speed
        if there are no neighbours around, return to cruising speed
        if there are neighbours in zone of repulsion
         *slow down
        elseif there are neighbours in zone of alignment
          *adjust speed to neighbours speed while trying to return to cruising speed
        elseif there are only neighbours far away
           *speed up to catch up with school
        if speed exceeds maximal acceleration, speed becomes maximum or minimum

        %make new position
        c_i(t+1)=c_i+s(i,t+1)*d_i(t+1)*dtau

        %check if new position does not exceed water surface
        or goes below the sea floor
        *adjust position

    end%end fishloop

plot 3D
plot xy
plot yz
plot xz
end%end timeloop


%plot horizontal and vertical angle distribution through time


%plot speed distribution through time
```

Appendix B

Suplementary material

CD/DVD with movies and full MATLAB code.

References

1. Barbaro, A., Elinarsson, B., Birbir, B., Sigurosson, S., Valdimarsson, H., Pálson, Ó.K., Sveinbjörnsson, S., Sigurosspn, P., 2009. modelling and simulations of the migration of pelagic fish. *ICES Journal of Marine Science*, 66, 826-838

2. Barbaro, A., Taylor, K., Trethewey, P.F., Youseff, L., Birnir, B., 2009. Discrete and continuous models of the dynamics of pelagic fish: Application to the capelin. *Mathematics and Computers in Simulation* 79, 3397-3414

3. Bejan, A., Marden, J.H., 2006. Unifying constructal theory for scale effects in running, swimming and flying. *Journal of Experimental Biology* 209, 238-248.

4. Birnir, B., 2007. An ODE Model of the Motion of Pelagic Fish. *Journal of Statistical Physics*, Vol. 128, Nos. 1/2, 535-567

5. Bone, Q., Moore, R.H., 2008, *Biology of Fishes.* Taylor and Francis Group, New York.

6. Brodersen, J., Nilsson P.A., Ammitzboll, J., Hansson, L-A., Skov, C., 2008. Optimal swimming speed in head currents and effects on distance movement of winter-migrating fish. *PLoS ONE* 3, 5, e1256.

7. Couzin, D., Krause, J., Franks, R.N., Levin, S.A., 2005. Effective leadership and decisionmaking in animal groups on the move. *Nature* 433, 513-516.

8. Hemelrijk, C.K., Kunz, H., 2003. Artificial fish schools: collective effects of school size, body size and body form. *Artificial Life* 9, 237-253.

9. Hemelrijk, C.K., Hildenbrandt, H., 2007. Self-organized shape and frontal density of fish schools. *Ethology* 114, 245-254.

10. Hubbard, S., Babak, P., Sigurdsson, S.T., Magnússon, K.G., 2004. A model of the formation of fish schools and migration of fish. *Ecol. Modelling* 174, 359-374.

11. Huth, A.,Wissel,C.,1992. The simulation of the movement of fish schools. *J. Theor. Biol,* 156, 365-385

12. Huth, A.,Wissel,C., 1994. The simulation of fish schools in comparison with experimental data. *Ecol. Modelling*75/76, 135-145.

13. Kibble, T.W.B., 1985. *Classical mechanics.* Longman Scientific & Technical, New York.

14. Krause,J., & Ruxton, G.D. 2002. *Living in groups.* Oxford Univ. Press, Oxford.

15. D'Orsogna, M.R., Chuang, Y., Bertozzi, A.L., Chayes, L.S., 2006. Pattern formation, stability and collapse in 2D driven particle system. *Device applications of nonlinear dynamics*, 103-115, edited by Bulsara, A. and Baglio, S. Springer-Verlag, Berlin Heidelberg.

16. D'Orsogna, M.R., Chuang, Y., Bertozzi, A.L., Chayes, L.S., 2006. Self-propelled particles with soft-core interactions: patterns, stability, and collapse. *PRT* 96, 104302

17. Parrish, J.K., Viscido, S.V., Grünbaum, D., 2002. Self-Organized Fish Schools: An Examination of Emergent Properties. *Biol. Bull.* 202: 296305.

18. Sfakiotakis, M., Lane, D.M., Bruce, J., Davies, C., 1999. Review of fish swimming modes for aquatic locomotion. *Journal of Oceanic Engineering* 24(2), 237-252.

19. Sparenberg, J.A., 2002. Survey of the mathematical theory of fish locomotion. *Journal of Engineering Mathematics* 44, 395-448.

20. Vicsek, T., Czirk, A., Ben-Jacob, E., Cohen, I.,Shochet, O. 1995. Novel Type of Phase Transition in a System of Self-Driven Particles. *Physical Review Letters* 75(6), 1226-1229.

21. Videler, J.J., 1993. *Fish Swimming.* Chapman and Hall, London.

22. Viscido, S., Miller, M., Wethley, D., 2002. The dilemma of the selfish herd: the search for a realistic movement rule. *J. Theor. Biol.* 217, 183-194.

23. Viscido, S., Parrish, J., Grünbaum, D., 2004. Individual behavior and emergent properties of fish schools: a comparison of observation and theory. *Mar. Ecol. Progr. Ser.* 273, 239-259.

24. Viscido, S.V., Parrish, J.K., Grünbaum, D., 2007. Factors influencing the structure and maintenance of fish schools. *Ecol. Modelling* 206, 153-165.